Functional models of [Fe—S] nitrosyl proteins

N. A. Sanina and S. M. Aldoshin*

Institute of Problems of Chemical Physics, Russian Academy of Sciences,
142432 Chernogolovka, Moscow Region, Russian Federation.
Fax: +7 (096) 524 9676. E-mail: sanina@icp.ac.ru

The review surveys methods for the synthesis, as well as structures and properties of sulfur-containing iron nitrosyl complexes serving as models of active sites of [Fe—S] nitrosyl proteins, which are potential donors of nitrogen monoxide.

Key words: synthesis, sulfur-containing iron nitrosyl complexes, heterocyclic thiols, NO donors, X-ray diffraction analysis, Mössbauer spectroscopy, magnetic susceptibility, cyclic voltammetry, ESR spectroscopy.

Introduction

In the last decade, the chemistry of [Fe—S] nitrosyl complexes has attracted attention because of an important role of nitrogen monoxide in bioregulation and immunology.[1—9] The main targets for NO *in vivo* are proteins containing, in active sites, metal ions that can easily coordinate this molecule,[10—12] and low-molecular-weight cellular substrates, such as superoxide anions, oxygen, amines, thiols, *etc.*[13—15] Reactions of these targets with NO produce peroxynitrite and other active NO_x species, which induce the formation of carcinogenic *S*-nitrosothiols and nitrosoamines in cells and are responsible for deamination of DNA bases and inhibition of DNA reparation.[16] Iron regulatory proteins play a key role in regulation of redox homeostasis. These proteins are activated by superoxide radicals, iron, and NO and affect, in particular, transcription of superoxide dismutase and a number of other anti-stress proteins. In a typical iron-sulfur regulon, the active site consists of two [2Fe—2S] clusters.[17—20] Nitrosyl complexes of non-heme proteins, along with low-molecular-weight *S*-nitroso derivatives of thiols (cysteine, glutathione, penicillamine, *etc.*), serve as stable NO biological reservoirs, which provide transport of nitrogen monoxide in cells of living organisms.[21—28] Proteins, such as glutathione transferase,[29] serve as natural depots for nitrogen monoxide.[30,31] Synthesis of and investigations into structural analogs of nitrosyl adducts of non-heme iron are of importance primarily from the standpoint of fundamental studies of the reaction mechanisms of endogenous NO. Studies of the mechanisms of action of reducing agents on model [Fe—S] nitrosyl clusters are of particular interest, because nitrosyl non-heme proteins in cells are involved in redox reactions with biological electron donors and antioxidants (NADP, cysteine, glutathione, ascorbate, Trolox C) and perform electron transport.[32,33]

Investigations into the structures and physicochemical properties of synthetic models of active sites of non-heme [Fe—S] nitrosyl proteins are related to application of knowledge in practice for the selective delivery of nitrogen monoxide *in vivo*.[34—45] In recent years, a search for, and studies of, new nitrogen monoxide donors have attracted considerable attention of experts in practical medicine. There are several classes of compounds that generate nitrogen monoxide during metabolic processes.

1. Nitrates, which are the most well-known NO donors (glycerol trinitrate, pentaerythritol tetranitrate, nicorandil, NO-aspirin, NO-paracetamol), are still most widely used for treating symptoms of stenocardia.[46—50] The efficiency of these pharmaceuticals depends on the metabolism of the nitro group.

2. Diazenium 1,2-diolates R—[N(O)—NO]$^-$ (NONOates). Depending on the nature of the substituent R (Et_2N, PrHN, SO_3^-, *etc.*), the half-lifes of these compounds vary from 2 s to 20 h.[51—54] This highly efficient class of NO donors does not require additional activation. However, NONOates are of limited use because of their high cost.

3. Morpholine derivatives of sydnonimines. One of such derivatives, *viz.*, molsidomine, is transformed during metabolism into the active metabolite SIN-1 possessing high vasodilatory activity.[55—57] However, these compounds eliminate nitrogen monoxide along with superoxide anions, resulting in the formation of carcinogenic peroxynitrite ($ONOO^-$) and the onset of pathogenic conditions *in vivo*.

4. *S*-Nitrosothiols (RSNO, where R is the cysteine, glutathione, or penicillamine residue) are formed *in vivo* as a result of the attack of nitrosonium ion on thiols. The

Published in Russian in *Izvestiya Akademii Nauk. Seriya Khimicheskaya,* No. 11, pp. 2326—2345, November, 2004.

1066-5285/04/5311-2428 © 2004 Springer Science+Business Media, Inc.

physicochemical properties of these compounds were studied in sufficient detail.[13,14] The decomposition rate depends on the nature of thiol. *S*-Nitrosothiols are of limited use because of their storage instability and cytotoxicity;[6] in the presence of redox agents, thiyl radicals and nitrosonium ions are formed. The former rapidly recombine to disulfides, and nitrosonium ions are hydrolyzed to form nitrite anions.

5. Cyanonitrosyl metallates with the composition $[M(CN)_xNO_y]^n$. In particular, sodium nitroprusside $Na_2[Fe(CN)_5NO]$ is, in certain cases, more efficient than diazenium 1,2-diolates.[58—62] Liberation of NO from the nitrosyl complexes requires photoactivation or chemical activation. This is accompanied by *in vivo* accumulation of cyanides, which limits the use of cyanonitrosyl metallates in clinical practice.[63]

6. Nitrosyl [Fe—S] complexes were discovered in nature in cells of microorganisms, plants, and mammalians. This class of NO donors remains poorly studied in spite of essential advantages of these complexes. The use of iron nitrosyl complexes with sulfur-containing ligands as adjuvants in chemo- and radiotherapy[48,64—66] opens up new prospects for the efficient treatment of malignant tumors. These compounds initiate synthesis of stress proteins, which enhance protective systems in organisms.[67] They can be used for the design of a new class of cardiovascular drugs, as animal tests have shown them to manifest a vasodilatory effect.[68—71]

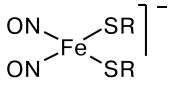

Mononuclear

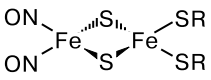

Dinuclear

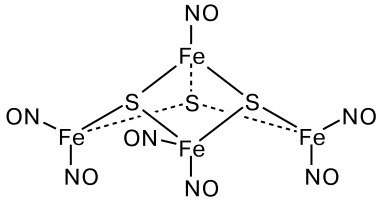

Tetranuclear

The present review covers the methods of synthesis and surveys structures and properties of di- and mononuclear [Fe—S] nitrosyl complexes, which are synthetic models of active sites of [2Fe—2S] and [1Fe—2S] nitrosyl proteins serving as natural reservoirs for nitrogen monoxide. These compounds, unlike toxic polynuclear [Fe—S] nitrosyl clusters (containing four or more iron atoms), hold promise as inorganic NO donors for biological and medical investigations.

Methods for the synthesis of [Fe—S] nitrosyl complexes

First synthetic analogs of non-heme iron-sulfur nitrosyl proteins, *viz.*, the "black" $[Fe_4S_3(NO)_7]^-$ and "red" $[Fe_2S_2(NO)_4]^{2-}$ salts, were synthesized[72] in 1858. Later, more perfect procedures for their synthesis appeared.[73]

$$FeSO_4 + NaNO_2 + (NH_4)_2S \xrightarrow{NH_4OH} NH_4[Fe_4S_3(NO)_7] \xrightarrow{MOH} M_2[Fe_2S_2(NO)_4] \xrightarrow{R_4NHal} (R_4N)_2[Fe_2S_2(NO)_4]$$

Photoactivation of both salts leads to NO elimination. However, experiments on cell cultures, the human neoplastic cell line (SK-MEL188), and the mouse neoplastic cell line (S91)[66] demonstrated that the "black" salt is cytotoxic.[7,36] Therefore, the use of tetranuclear iron-sulfur clusters as NO donors is of no practical interest.[43,74] Roussin's red salt is less toxic and more photoactive. However, this salt as an NO donor is of limited use because it is very unstable. In solutions, this complex is transformed into the "black" salt.[73,75,76]

$$2\,H^+ + 4\,Fe_2S_2(NO)_4^{2-} \xrightarrow{h\nu} 2\,Fe_4S_3(NO)_7^- + 2\,S^{2-} + N_2O + H_2O$$

Cyclic voltammograms of the tetrabutylammonium complexes of the "black" (Fig. 1, *a*, curve *1*) and "red" salts (curve *2*)[76] are virtually identical both in shape and peak potentials (Table 1). In solutions, the dianion immediately decomposes followed by the formation of the tetranuclear complex $[Fe_4S_3(NO)_7]^-$. Quantum-chemical calculations demonstrated[73] that in the cluster with the tetranuclear anion, the lowest unoccupied molecular orbital composed primarily of the orbitals of the Fe—Fe bond is antibonding. Nevertheless, one-electron reduction of this anion is reversible, which suggests that the $[Fe_4S_3(NO)_7]^{\bullet 2-}$ radical dianion is stable, at least on the CV time scale. The overall two-electron reduction of the anion of Roussin's black salt is irreversible. This indicates that the transfer of the second electron to the cluster causes substantial structural rearrangements, resulting presumably in the destruction of the cluster core. Thus, the reduction mechanism can be written as follows:

$$[Fe_4S_3(NO)_7]^- + e \rightleftharpoons [Fe_4S_3(NO)_7]^{\bullet 2-} + e \longrightarrow [Fe_4S_3(NO)_7]^{3-} \longrightarrow \text{Products.}$$

Unlike the "red" salt, the so-called Roussin red salt esters are more stable. The method for their preparation is based on the reaction of Roussin's red salt with alkyl halides.[77—80]

$$[Fe_2S_2(NO)_4]^{2-} + 2\,RHal \longrightarrow [Fe_2(SR)_2(NO)_4]$$

R = Me, Et, CH_2Ph, CH_2CH_2OH, $CH_2CH_2SO_3^-$

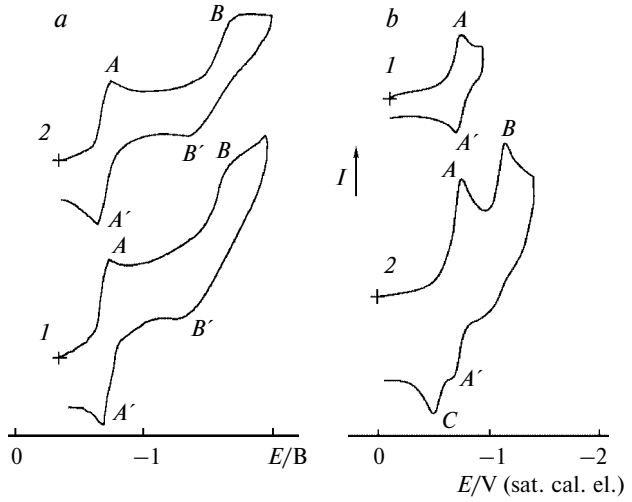

Fig. 1. *a*, Cyclic voltammograms of the complexes with the $[Fe_4S_3(NO)_7]^-$ monoanion (curve *1*) and the $[Fe_2S_2(NO)_4]^{2-}$ dianion (curve *2*) in THF—0.1 *M* Bu_4NPF_6 on a Pt electrode (v = 0.2 V s^{-1} at 20 °C); *b*, cyclic voltammograms of the complexes with the $[Fe_2(S_2O_3)_2(NO)_4]^{2-}$ dianion (curve *1*, one-electron reduction; curve *2*, two-electron reduction) in MeCN—0.05 *M* Bu_4NPF_6 on a glassy-carbon electrode (v = 0.2 V s^{-1} at 20 °C).

Table 1. Potentials of the reduction peaks of Roussin's black salt ($[Fe_4S_3(NO)_7]^-$) and Roussin's red salt ($[Fe_2S_2(NO)_4]^{2-}$) (relative to a saturated calomel electrode) in MeCN—0.05 *M* Bu_4NPF_6 (an Au electrode) and THF—0.1 *M* Bu_4NPF_6 (a Pt electrode) at v = 0.2 V s^{-1} and T = 20±2 °C

Complex with anion	Peak	E^0 (E_p^c)	
		MeCN	THF
$[Fe_4S_3(NO)_7]^-$	*A*/*A*´	−0.72	−0.93
	B	(−1.68)	(−1.74)
	B″	(−1.32)	(−1.44)
$[Fe_2S_2(NO)_4]^{2-}$	*A*/*A*´	−0.72	−0.94
	B	(−1.72)	(−1.69)
	B″	(−1.30)	(−1.43)

The reactions of sulfur-containing ligands (thioglycolate, 2-mercaptoethanol, 2-methylpropane-2-thiol) with $NaNO_2$ and $FeSO_4$ also afford neutral dinuclear nitrosyl complexes.[81] These compounds are isostructural to the iron thiosulfate nitrosyl complex, which was prepared for the first time[82] in 1895 in a yield of up to 65% according to the scheme

$$2\,FeSO_4 + 4\,K_2S_2O_3 + 4\,NO \longrightarrow$$
$$\longrightarrow K_2[Fe_2(S_2O_3)_2(NO)_4] + K_2S_4O_6 + 2\,K_2SO_4$$

Later, $NaNO_2$ was used as the nitrosating agent.[83] However, this method appeared to be less efficient, because the reaction afforded iron(III) hydroxide as the by-product, and the nitrosyl product was prepared in 30% yield.

The cyclic voltammogram of the thiosulfate complex (see Fig. 1, *b*)[84] shows two cathodic peaks *A* and *B* with nearly equal heights. Stepwise two-electron reduction of this compound is completely reversible in the first step, which followed from the equality of both the cathodic (*A*) and anodic (*A*´) peaks (see Fig. 1, *b*, curve *1*) and the difference $\Delta E_p = E_p^a - E_p^c$ (E_p^c and E_p^a are the potentials of the cathodic (*A*) and anodic (*A*´) peaks), which is equal to 60—65 mV both in CH_2Cl_2 and MeCN. The equality of the heights of the peaks *A* and *A*´ is indicative of stability of the one-electron reduction product (a trianion). Further one-electron reduction of the mixed-valence Fe^0Fe^I complex is reversible (see Fig. 1, *b*, curve *2*, peak *B*), which provides evidence for instability of the resulting tetraanion. Its decomposition product is oxidized at potentials of the peak *C*, which appears in the anodic branch of the voltammogram only after the potential of the peak *B* is achieved. The presence of the peak *C* suggests that the Fe^0Fe^0 tetraanion is unstable. Thus, the reduction of the thiosulfate nitrosyl complex can be represented by the following scheme:

$$[Fe_2(\mu\text{-}S_2O_3)_2(NO)_4]^{2-} + e \rightleftharpoons$$
$$\rightleftharpoons [Fe_2(\mu\text{-}S_2O_3)_2(NO)_4]^{3-} + e \longrightarrow$$
$$\longrightarrow [Fe_2(\mu\text{-}S_2O_3)_2(NO)_4]^{4-} \longrightarrow \text{Products.}$$

The reactions of the mononuclear thiosulfate nitrosyl complex with the corresponding thiols gave "esters," where R = Me, Et, Pr^i, Pr^n, Bu^i, Bu^n, or $(CH_2)_4Me$,[85] according to the scheme:

$$[Fe_2(S_2O_3)_2(NO)_4]^{2-} + 2\,S_2O_3^{2-} \longrightarrow$$
$$\longrightarrow 2\,[Fe(S_2O_3)_2(NO)_2]^{3-} + 2\,RS^- \longrightarrow$$
$$\longrightarrow 4\,S_2O_3^{2-} + [Fe_2(SR)_2(NO)_4].$$

Nitrosyl complexes were isolated from the reaction mixture in yields of up to 60%. Unfortunately, this method is inapplicable to CH_2Cl_2-insoluble complexes. Complexes $[Fe_2(SR)_2(NO)_4]$ can also be synthesized according to Brauer's method[86] in yields of up to 80%. However, this reaction gives rise to Fe_2O_3 and, hence, this procedure is inapplicable to thiols with low basicities (pK_a):

$$4\,FeSO_4 + 8\,KOH + 2\,RSH + 4\,NO \longrightarrow$$
$$\longrightarrow [Fe_2(SR)_2(NO)_4] + 4\,K_2S_2O_4 + Fe_2O_3 + 5\,H_2O$$

Neutral "esters" can also be prepared by the reaction of AlkSH with the $[Fe_2I_2(NO)_4]$ complex in the presence of weak bases[87] or by the reaction of Alk_2S_2 with the carbonyl complex $[Fe(CO)_2(NO)_2]$.[25] Studies by ESR spectroscopy demonstrated that these reactions proceed *via* mononuclear iron dinitrosyl complexes (IDNC).[88]

The quantum yields of the reactions resulting in elimination of NO from Roussin's salt esters containing alkyl

substituents are 0.02—0.13. Recent studies[89] demonstrated that one mole of the complex gives 4 moles of NO, unlike the "black" salt, which generates 3.7 moles of NO per mole of the salt.[66] Data on cytotoxicity of these compounds are lacking in the literature, except for information[73] on the carcinogenic properties of the neutral dinuclear complex $[Fe_2(SMe)_2(NO)_4]$.

Mononuclear iron dinitrosyl complexes with natural thiols (cysteine, glutathione, *etc*.) are presently used as stable [Fe—S] donors of NO in biochemical and medical studies. Such complexes were prepared by passing NO through a mixture of iron(II) sulfate and the corresponding thiol in a molar ratio of 1 : 2.[22,90—94] No mononuclear iron dinitrosyl complexes with natural ligands have been isolated in the crystalline state so far. It is known that iron nitrosyl complexes exist *in vivo* in mononuclear $[Fe(SR)_2(NO)_2]^-$ and dinuclear $[Fe_2(SR)_2(NO)_4]$ forms.[95—97] These forms exist in dynamic equilibrium, which depends on the concentration of thiols in physiological conditions. Mononuclear iron dinitrosyl complexes are identified in solutions based on the characteristic ESR signal with g ≈ 2.03. The first synthetic analog of IDNC with a sulfur-containing ligand has the anionic structure $[NEt_4][Fe(NO)_2(SPh)_2]$ [98] and was prepared by the reaction of Roussin's black salt with diphenyl disulfide according to the scheme

$$[Fe_4S_3(NO)_7]^- \xrightarrow{i} (Et_4N)[Fe(SPh)_2(NO)_2]$$

i. PhSSPh/KOH, 110 °C; Et_4NCl/MeOH.

Later, a [1Fe—2S] dinitrosyl complex was prepared by the reaction of $(FeL)_2$, where L is the *N*,*N*-dimethyl-*N*,*N*-bis(2-mercaptoethyl)propane-1,3-diamine dianion, with $NOPF_6$ in dichloromethane.[99]

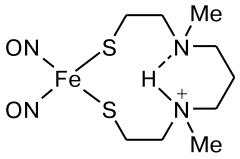

Because of *in vitro* instability, mononuclear iron dinitrosyl complexes are very difficult to crystallize,[24] and the structures and physicochemical properties of these complexes are difficult to study. Recent extensive studies made it possible to isolate and characterize single crystals of new [Fe—S] dinitrosyl complexes with the use of *N*,*N*′-bis(2-mercaptoethyl)-1,5-diazacyclooctane (H_2bme-daco)[100] according to the scheme

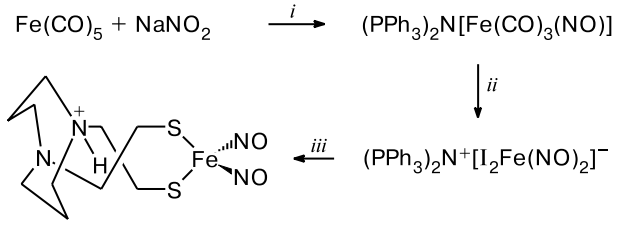

i. Na^0/THF, $[N(PPh_3)_2]Cl$/MeOH; *ii*. I_2/THF; *iii*. H_2bme-daco, THF, 0 °C.

The resulting complex is stable at −35 °C. Storage of the mononuclear iron complex in solution in air or an increase in the temperature as well as the presence of moisture lead to its decomposition.

There is no consensus on the structures and properties of dinuclear [Fe—S] nitrosyl complexes, and these questions are actively discussed in the literature. For example, it was hypothesized[101,102] that the dinuclear iron complexes $[Fe_2(SR)_2(NO)_4]$ exist in solution as dimeric associates of the mononuclear iron dinitrosyl complexes.

Therefore, a search for new synthetic iron nitrosyl thiolates and study of their properties are necessary for understanding of the true structures of these compounds. We synthesized a stable mononuclear complex by the reaction of the iron thiosulfate nitrosyl complex with 1*H*-1,2,4-triazole-3-thiol according to the following scheme:[103]

$$n\,[Fe_2(S_2O_3)_2(NO)_4]^{2-} + 2n\,S_2O_3^{2-} \longrightarrow$$

$$\longrightarrow 2n\,[Fe(S_2O_3)_2(NO)_2]^{3-} \longrightarrow$$

$$\xrightarrow[-2n\,S_2O_3^{2-}]{+10n\,STriaz^-,\ 4n\,OH^-} n\,[Fe(STriaz)_2(NO)_2].$$

We proposed to use the following bidentate nitrogen-containing heterocyclic thiols[103—105] as ligands for the synthesis of dinuclear [Fe—S] nitrosyl complexes:[104,105] pyridine-2-thiol (**1**), pyrimidine-2-thiol (**2**), benzothiazole-2-thiol (**3**), benzimidazole-2-thiol (**4**), 1*H*-1,2,4-triazole-3-thiol (**5**), 5-amino-1,2,4-triazole-3-thiol (**6**), and 1-methyltetrazole-5-thiol (**7**). These ligands possess a high coordination potential[106—108] due to the presence of the μ-N—C—S structural fragment. The functional properties of the complexes can be varied depending on the nature of the ligand used.

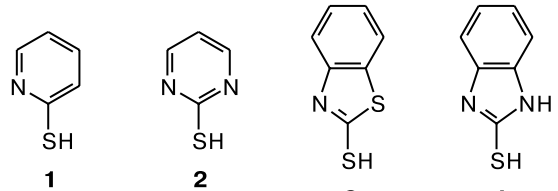

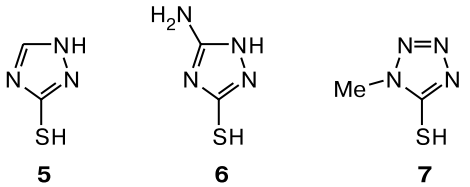

The method, which we have developed for the synthesis of such complexes, is based on the exchange of the thiosulfate ligands in iron dinitrosyl complexes[84] for the

hetarylthio ligands in physiological conditions according to the scheme

$$[Fe_2(S_2O_3)_2(NO)_4]^{2-} + n\ S_2O_3^{2-} \longrightarrow$$

$$\longrightarrow n\ [Fe(S_2O_3)_2(NO)_2]^{3-} \xrightarrow[-2n\ S_2O_3^{2-}]{+2n\ RS^-,\ n\ OH^-}$$

$$\longrightarrow n\ [Fe_2(SR)_2(NO)_4] + n\ SR^-.$$

The synthesis of [Fe—S] nitrosyl complexes with azaheterocyclic thiols is of importance from the standpoint of studies of the coordination modes of iron by the thiol in the presence of NO. The ligand can be coordinated to the iron atom in a *monodentate fashion* through either the sulfur atom, η^1-S (I), or the nitrogen atom, η^1-N (II), in a *bridging fashion* through either the sulfur atom, μ_2-S (η^2-S) (III), or the sulfur and nitrogen atoms, μ_2-S, N (η^2-S; η^1-N) (IV), in a *chelate fashion*, μ_1-S,N (η^1-S, η^1-N) (V), and in *combined fashions*, μ_3-S,N (η^2-S, η^1-N) (VI), and μ_2-S,N (η^2-S, η^1-N) (VII).[108]

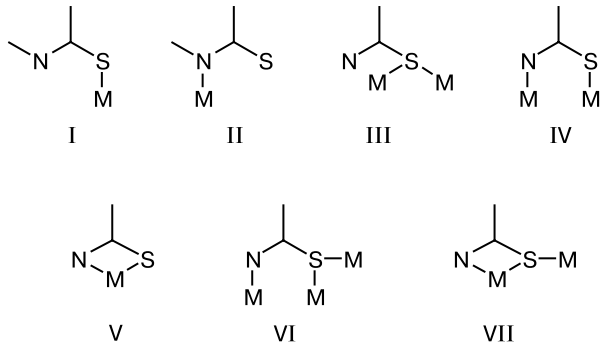

Besides, the presence of substituents (NH_2, COOH, OH, *etc.*) in heterocyclic thiols can additionally extend the coordination potential of the ligand. Tautomerism[107] and, correspondingly, the presence of the tautomer **A** or **B** or sometimes of their mixture affects substantially the coordination mode of the heterocyclic ligand in the metal—ligand bonding.

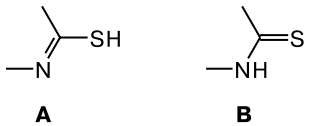

Compounds prepared according to this procedure serve as models of non-heme iron nitrosyl complexes and contain simultaneously two functional fragments, *viz.*, NO and RS. Of thiols **1—7** exhibiting antibacterial and inhibiting activities, benzimidazole-2-thiol (**4**) and benzothiazole-2-thiol (**3**) are of interest. The former serves as a cAMP phosphodiesterase inhibitor, and the latter is a polyphenol oxidase inhibitor exhibiting antimicrobial properties.[109] Triazole- and tetrazolethiols possess a broad spectrum of antimicrobial and fungicidal properties, block the formation of ribosomes and DNA, and inhibit riboflavin biosynthesis.[110—113] It is known that pyridine-2-thiol (**2**) serves as a potent antimetabolite of pyrimidine bases of nucleic acids. Its pharmacological action is analogous to that of 6-thioguanine and 6-mercaptopurine, which are used in clinical practice for the treatment of acute leukemia. For example, an antineoplastic effect was manifested by coordination compounds of metals with pyridine- and pyrimidinethiols.[114—117]

Structures of [Fe—S] nitrosyl complexes

The anion of the $NH_4[Fe_4S_3(NO)_7]\cdot H_2O$ complex can be described as a trigonal pyramid,[76] whose vertices are occupied by iron atoms (Fig. 2, Table 2). The ideal symmetry of the anion is C_{3v}. The distances between the Fe atoms can be characterized by two types of contacts: (1) the contacts between the apical atom Fe_a (Fe(1)) and the atoms forming the base of the pyramid, Fe_b (Fe(2), Fe(3), and Fe(4)) (Fe(1)—Fe(2), 2.693(1) Å; Fe(1)—Fe(3), 2.696(1) Å; Fe(1)—Fe(4), 2.707(1) Å), and (2) the contacts between the atoms of the base of the pyramid Fe_b (Fe(2)—Fe(3), 3.601(1) Å; Fe(2)—Fe(4), 3.543(1) Å; Fe(3)—Fe(4), 3.563(1) Å). The Fe_b atoms in the base of the pyramid are linked through the sulfur bridges Fe_b—S—Fe_b. The sulfur atoms of these bridges form bonds with the apical Fe_a atom as well. The average Fe_a—S and Fe_b—S distances (2.205(1) and 2.256(2) Å, respectively) are consistent with the data published in the literature[118,119] (2.206 and 2.258 Å, respectively). The apical Fe(1) atom (Fe_a) is bound to one NO ligand and three bridging S atoms, whereas each Fe_b atom (Fe(2), Fe(3), and Fe(4)) is coordinated by two nitrosyl ligands and two bridging S atoms.

Analysis of the bond lengths in the nitrosyl ligands (Table 3) shows that the Fe_a—N bond (1.651(2) Å) is shortened compared to the analogous Fe_b—N bonds in-

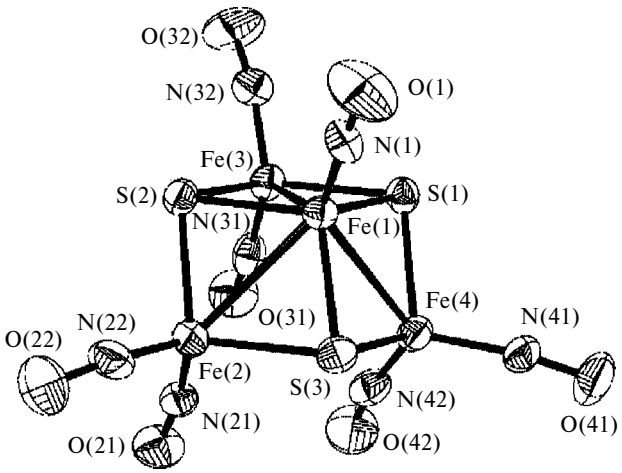

Fig. 2. Crystal structure of the anion of Roussin's black salt: Fe(1) = Fe_a; Fe(2), Fe(3), Fe(4) = Fe_b.

Table 2. Main crystallographic data for single crystals of iron-sulfur nitrosyl complexes

Complex	Molecular weight	Crystal system	Space group	*a*, [*b*], {*c*} / Å	α, [β], {γ} / deg	V/Å^3	Z	d /g cm^{-3}	Reference
$NH_4[Fe_4S_3(NO)_7]\cdot H_2O$	565.46	Triclinic	$P\bar{1}$	9.451(2) [10.000(2)] {10.577(2)}	59.02(3) [68.57(3)] {79.05(3)}	797.9(3)	2	2.353	76
$Cs_2[Fe_2S_2(NO_4]\cdot 2H_2O$	597.71	Monoclinic	$P2_1/c$	9.608(2) [11.402(2)] {12.601(3)}	90 [107.13(3)] {90}	1319.2(5)	4	3.009	76
$(Pr^n{}_4N)_2[Fe_2S_2(NO)_4]$	452.39	Monoclinic	$P2_1/n$	10.455(2) [13.647(1)] {12.504(3)}	90 [92.02(3)] {90}	1781.6(7)	2	1.246	123
$(Me_4N)_2[Fe_2(S_2O_3)_2(NO)_4]$	604.09	Triclinic	$P\bar{1}$	7.719(2) [12.272(2)] {6.513(1)}	83.78(3) [86.30(3)] {73.48(3)}	587.6(2)	1	1.708	122
$(Bu^n{}_4N)_2[Fe_2(S_2O_3)_2(NO)_4]$	868.32	Monoclinic	$P2_1/c$	20.332(4) [13.070(3)] {18.009(4)}	90 [91.07(3)] {90}	4785(2)	4	1.205	83
$[Fe_2(SC_5H_4N)_2(NO)_4]$	443.98	Monoclinic	$C2/c$	20.935(4) [7.964(2)] {13.697(3)}	90 [132.65(3)] {90}	1679.6(6)	4	1.756	124
$[Fe_2(SC_4H_3N_2)_2(NO)_4]$	454.03	Triclinic	$P\bar{1}$	7.675(1) [8.423(1)] {6.447(1)}	80.93(1) [85.42(1)] {75.06(1)}	397.3(1)	1	1.898	125
$[Fe_2(SC_2H_3N_4)_2(NO)_4]\cdot 2H_2O$	479.95	Triclinic	$P\bar{1}$	8.006(2) [7.809(2)] {8.471(3)}	64.42(3) [71.46(3)] {67.01(3)}	432.6(2)	1	1.912	105
$[Fe(SC_2H_3N_3)(SC_2H_2N_3)(NO)_2]\cdot 0.5H_2O$	326.14	Monoclinic	$C2/c$	18.789(4) [9.528(2)] {13.623(3)}	90 [99.73(3)] {90}	2403.7(9)	8	1.802	103

volving the peripheral atoms (1.661(6)—1.675(7) Å). All Fe—N—O fragments are nearly linear; the equatorial angles are 169.4(1), 171.2(1), and 166.4(1)° (*cf.* lit. data[118,119]: 167.5°). The axial angles in the $[Fe_4S_3(NO)_7]^-$ anion are 166.9(1), 166.9(1), and 168.0(1)° (*cf.* lit. data[118,119]: 166.1°), *i.e.*, these angles are smaller than the Fe_a—N—O angle (176.5(1)°; *cf.* lit. data[118,119]: 176.3°). The differences in the bond angles are apparently associated with the formation of intermolecular NH_4^+...ON ($N(NH_4^+)$...O(21), 3.10 Å; ($N(NH_4^+)$...O(21′), 3.15 Å)

Table 3. Selected average bond lengths (d) and bond angles (ω) in [Fe—S] nitrosyl complexes

Complex	d/Å				ω/deg		Reference
	N—O	Fe—N	Fe—S	Fe—Fe	Fe—N—O	N—Fe—N	
$NH_4[Fe_4S_3(NO)_7]\cdot H_2O$	1.160 ($N—O)_a$ 1.166 ($N—O)_b$	1.651 ($Fe_a—N$) 1.669 ($Fe_b—N$)	2.205 ($Fe_a—S$) 2.256 ($Fe_b—S$)	2.697 ($Fe_a—Fe_b$) 3.569 ($Fe_b—Fe_b$)	176.5 ($Fe_a—N—O$) 168.1 ($Fe_b—N—O$)	116.8 ($N—Fe_b—N$)	76
$Cs_2[Fe_2S_2(NO)_4]\cdot 2H_2O$	1.148—1.175	1.654—1.675	2.230—2.240	2.700—2.720	163.8—167.9	112.3—114.9	76
$\{Pr^n{}_4N\}_2[Fe_2S_2(NO)_4]\cdot 2H_2O$	1.176—1.179	1.650—1.655	2.224—2.226	2.704	163.2—163.5	111.5	124
$\{Me_4N\}_2[Fe_2(\mu_2\text{-}S_2O_3)_2(NO)_4]$	1.150—1.170	1.664—1.675	2.257—2.260	2.70	168.0—171.3	115.6	123
$\{Bu^n{}_4N\}_2[Fe_2(\mu_2\text{-}S_2O_3)_2(NO)_4]$	1.149—1.170	1.666—1.669	2.250—2.251	2.702	167.5—170.8	117.1—117.6	122
$[Fe_2(SC_5H_4N)_2(NO)_4]$	1.125—1.190	1.640—1.660	2.280	2.725	170.9—171.7	119.4	125
$[Fe_2(SC_4H_3N_2)_2(NO)_4]$	1.131—1.174	1.650—1.684	2.249—2.269	2.726	166.7—172.5	117.1—119.5	126
$[Fe_2(SC_2H_3N_4)_2(NO)_4]\cdot 2H_2O$	1.149—1.157	1.669—1.677	2.298—2.318	4.040	168.2—171.5	118.7	105
$[Fe(SC_2H_3N_3)(SC_2H_2N_3)(NO)_2]\cdot 0.5H_2O$	1.183—1.170	1.658—1.682	2.311	5.225	158.1—171.5	112.5	103

and $H_2O...ON$ ($O(H_2O)...O(21)$, 2.99 Å; $O(H_2O)...O(21')$, 3.11 Å; $O(H_2O)...O(41)$, 3.10 Å) hydrogen bonds. Interestingly, the N(31)—Fe(3)—N(32) bond angle (119.1(1)°) is larger than two other bond angles (N(21)—Fe(2)—N(22), 115.6(1)°; N(41)—Fe(4)—N(42), 115.7(1)°). This change in the geometry is apparently attributable to the formation of a chain of intermolecular $NH_4^+...O(32)$ (N...O, 3.25 Å) and $NH_4^+...O(31)$ (N...O, 3.15 Å) hydrogen bonds, which "stretch" the nitrosyl ligands at the Fe(3) atom, thus causing the observed increase in the bond angle. Apparently, the complexes with the $[Fe_4S_3(NO)_7]^-$ anion are stabilized by three-center bonds formed by the bridging sulfur atoms.

The dianion of the $Cs_2[Fe_2S_2(NO)_4]$ [76] complex (Fig. 3), like those in isostructural salts with the Me_4N^+ [120] and Et_4N^+ [121] cations, has the approximate D_{2h} symmetry. Two iron atoms are linked through two bridging S atoms. The bridging S atoms in the dianion, in contrast to those in the tetranuclear anion, form bonds only with two Fe atoms. The Fe atoms are coordinated by two bridging S atoms and two NO ligands. The Fe—N—O fragments are linear. The Fe—N—O angles are in a range of 164(1)—168(1)°, which is similar to the range of the Fe_b—N—O angles in the anion of Roussin's black salt.

A decrease in the bond lengths in the $[Fe_2S_2(NO)_4]^{2-}$ dianion compared to those in the dianions of the complexes described earlier[10,120—122] (Fe—S, 2.232(3)—2.243(2) Å (2.239—2.250 Å for Me_4N^+; 2.239 and 2.241 Å for Et_4N^+, and 2.2245(2) Å for $Pr^n_4N^+$); Fe—Fe, 2.702(2) Å (2.713 and 2.716 Å for Me_4N^+; 2.713 Å for Et_4N^+, and 2.704 Å for $Pr^n_4N^+$)) is apparently attributable to the fact that the Cs^+ cation is smaller than tetraalkylammonium cations, resulting in a decrease in the degree of electron density transfer from the highest occupied molecular orbital of the anion to the cation in the cesium complex. These changes in the geometry of the anion can be adequately described at the extended Hückel theory level (EHMO).[73]

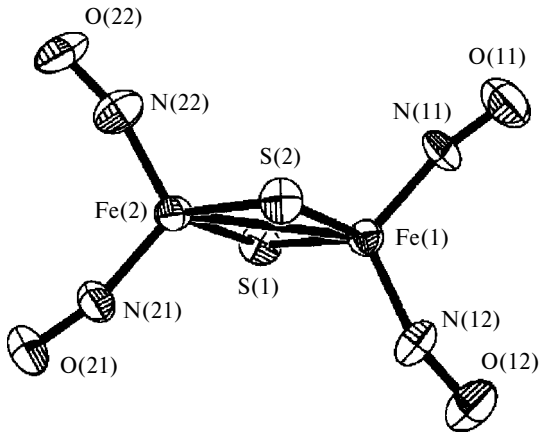

Fig. 3. Crystal structure of the anion of Roussin's red salt.

The difference between the N(11)—Fe(1)—N(12) and N(21)—Fe(2)—N(22) bond angles (114.7(4)° and 112.7(4)°, respectively) is associated with nonequivalence of the crystal environment. Analysis of the intermolecular Cs...N contacts showed that the environment of the N(11) atom (Cs(1)...N(11), 3.35 Å) differs substantially from those of the other nitrogen atoms (Cs...N, 3.49—3.77 Å). Analysis of the Cs...O intermolecular contacts revealed two pairs of nitrosyl ligands, which are in an approximately equivalent crystal environment.

Analysis of the crystal packing shows that the coordination number of Cs^+ is 12, and the $Cs^+...L$ distances (L is the ligand) are in ranges of 3.165(11)—3.725(13) and 3.112(10)—3.719(11) Å for Cs(1) and Cs(2), respectively. However, analysis of the Cs...Cs contacts demonstrated that these contacts in the crystal (Cs(1)—Cs(1), 4.285 Å; Cs(2)—Cs(1), 4.738 and 5.664 Å; Cs(2)—Cs(2), 4.832 Å) are shorter than the metal—metal bond (5.440 Å). Apparently, the positive charge in the crystal is only partially localized on the Cs atoms; otherwise, such Cs...Cs contacts in the crystal would be impossible.

In the diamagnetic dinuclear μ_2-S-substituted thiosulfate complexes (Fig. 4), the bridging sulfur atom is

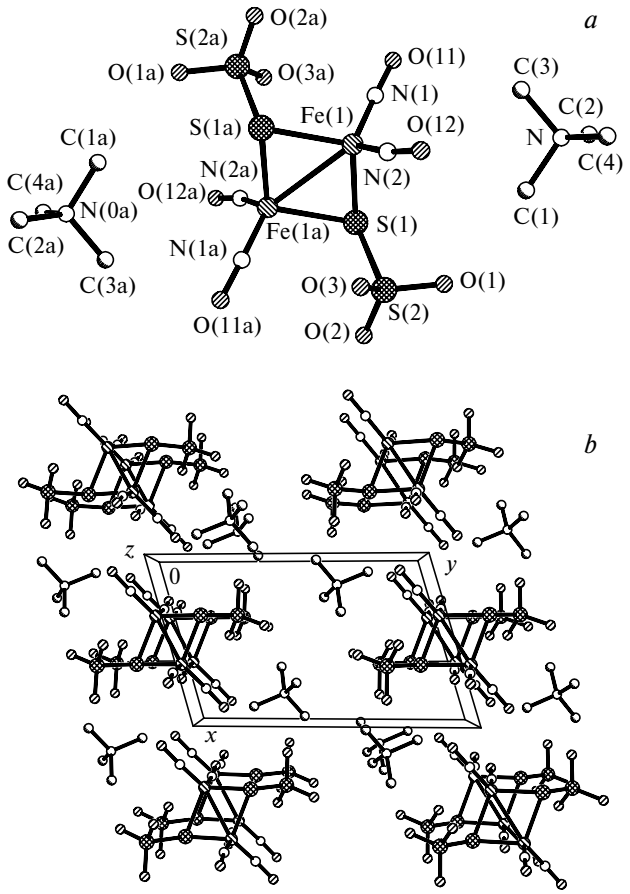

Fig. 4. Crystal structure (*a*) and the packing of the anions and cations of the $[(CH_3)_4N]_2[Fe_2(S_2O_3)_2(NO)_4]$ complex (*b*).

linked with the SO_3 group.[81,84,122] The distribution of the bond lengths in this series of compounds is similar to that in the tetranuclear Fe_b complexes. In the dinuclear centrosymmetric $[Fe_2(S_2O_3)_2(NO)_4]^{2-}$ anion, each metal atom is bound to another iron atom, two μ-sulfur atoms, and two nitrogen atoms of two NO groups. The dianions are packed in translational stacks along the *z* axis. The molecules of the adjacent stacks are linked through dipole-dipole interactions (N(1)—O(11′) and O(11a)—N(1a′), 3.34 Å), resulting in the formation of blocks along the *x* axis. The channels of the anion blocks formed by the negatively charged oxygen atoms of the SO_3 groups are occupied by the tetramethylammonium cations (N—O(1), N—O(2), and N—O(3), 3.7—3.9 Å). Apparently, the presence of the negatively charged SO_3 groups at the bridging sulfur atoms leads to the electron density distribution in the thiosulfate complexes compared to the sulfide $[Pr^n_4N]_2Fe_2S_2(NO)_4$ complex.[123] The SO_3 groups in the $[Fe_2(S_2O_3)_2(NO)_4]^{2-}$ anion sterically hinder the transformation of the dinuclear complex into the tetranuclear $[Fe_4S_3(NO)_7]^-$ complex. The thiosulfate complexes are more storage-stable in the dark and in the absence of moisture than the corresponding sulfide complexes, which is confirmed by IR and Mössbauer spectroscopic data. Simulation of the dimerization process demonstrated that short Fe—NO and Fe—SO_3 contacts (<2 Å) appear when the atoms approach each other to distances sufficient for the formation of Fe—S bonds.

In the presence of NO, nitrogen-containing heterocyclic thiols, *viz.*, pyridine-2-thiol (**1**) and pyrimidine-2-thiol (**2**), also form dinuclear μ_2-S-substituted iron complexes (Fig. 5).[124,125] The geometry of the complexes with ligands **1** and **2** is similar to that of iron thiosulfate nitrosyls[122,123] and the neutral $[Fe_2(\mu\text{-}SR)_2(NO)_4]$ complexes (R = Me, Et, *n*-C_5H_{11}, Bu^t).[80]

In the complex with ligand **1**,[124] two iron atoms (Fe and Fe_a) coordinated by the NO groups are linked to form a dimer through the bridging S and S(0a) atoms. The distances from the N(3) and N(3a) atoms of the pyridine ring to the Fe and Fe_a atoms are ~3.4 Å, which indicates that there are no coordination bonds between the iron atoms and the pyridine nitrogen atoms. Thus, pyridine-2-thiol manifests the coordination mode III. A comparison of the interatomic distances in the complex with ligand **1** and in other related compounds[80] revealed no substantial differences. Analysis of the crystal packing shows that there are two types of shortened intermolecular contacts: 1) the intermolecular contact between the "nonequivalent" NO groups (N(1)—O(1), 1.13(2) Å; N(2)—O(2), 1.19(2) Å) (intermolecular N(1)...O(2′) and O(2)...N(1′) distances are 3.15 Å) and 2) the intermolecular C(3)—H(3)...O(2) contact (O(2)...H(3), 2.42 Å; C(3)...O(2), 3.36 Å). It should be noted that only one hydrogen atom (H(3)) was revealed from the electron density map, this being involved in the interaction with the NO group,

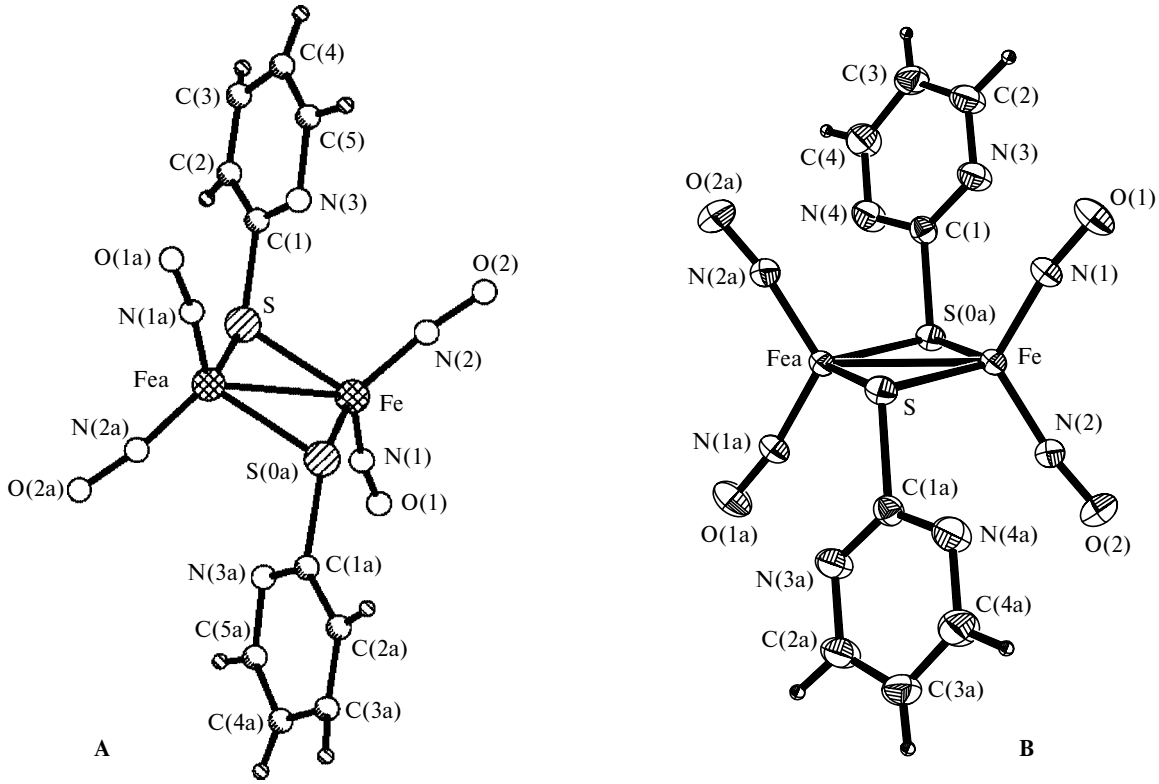

Fig. 5. Crystal structures of $[Fe_2(SC_5H_4N)_2(NO)_4]$ (**A**) and $[Fe_2(SC_4H_3N_2)_2(NO)_4]$ (**B**).

where the N—O bond is slightly longer (N(2)—O(2), 1.19(2) Å).

In the complex with ligand **2**,[125] the sulfur atoms also have a pyramidal configuration. The sums of the bond angles at the S(1) and S(2) atoms are 288.8° and 289.2°, respectively. As a result, the pyrimidine ring N(7)N(8)C(5)...C(8) is in the *syn* orientation with the nitrosyl groups N(2)O(2) and N(3)O(3) on the same side of the planar central Fe(1)Fe(2)S(1)S(2) fragment, and the pyrimidine ring N(5)N(6)C(1)...C(4) is in the *syn* orientation with the nitrosyl groups N(1)O(1) and N(4)O(4) on the opposite side of this fragment. The pyrimidine rings in the complex with ligand **2** are located nonsymmetrically with respect to the iron atoms in contrast to the complex with ligand **1**, where the nitrogen atom of the pyridine ring are located at equal distances from the iron atoms (~3.4 Å). The Fe(1)—S(2)—C(5)—N(7) and Fe(2)—S(1)—C(1)—N(5) torsion angles (20.3° and −26.4°) are smaller than the Fe(2)—S(2)—C(5)—N(8) and Fe(1)—S(1)—C(1)—N(6) torsion angles (82.8° and 79.6°, respectively). In spite of the fact that the intramolecular Fe(1)...N(7) and Fe(2)...N(5) distances (3.418(6) and 3.476(6) Å) in this structure are shorter than the Fe(1)...N(6) and Fe(2)...N(8) distances (3.672(6) and 3.707(6) Å), the former distances are rather long and indicate that the iron atoms are not additionally coordinated by the nitrogen atoms of the pyrimidine rings. However, this arrangement of the pyrimidine rings leads to shortening of the intramolecular N...N distances between the pyrimidine rings and nitrosyl groups (N(7)...N(2), 2.979(8) Å; N(5)...N(4), 3.026(8) Å). The NO groups are structurally different. Two Fe—N—O fragments have shorter N—O bonds (N(4)—O(4), 1.141(8) Å; N(1)—O(1) 1.155(7) Å), are less linear (Fe(2)N(4)O(4), 166.3(7)°; Fe(1)N(1)O(1), 167.6(5)°), and are located on the same side of the plane of the central fragment. Two other Fe—N—O fragments have longer N—O bonds (N(2)—O(2), 1.167(8) Å; N(3)—O(3), 1.174(8) Å), are more linear (Fe(1)—N(2)—O(2), 172.9(6)°; Fe(2)—N(3)—O(3), 171.1(7)°), and are located on the opposite side of the plane of the iron-sulfur ring. Taking into account high accuracy of X-ray diffraction and IR spectroscopic data, these small differences can be considered as physically meaningful. A shortening of the N—O bonds is accompanied by an elongation of the Fe—N bonds (Fe(2)—N(4), 1.702(5) Å; Fe(1)—N(1), 1.701(5) Å) compared to the Fe(1)—N(2) and Fe(2)—N(3) bonds (1.642(5) and 1.637(7) Å, respectively). The Fe—S and Fe—Fe bonds are only slightly longer than the analogous bonds in the complexes described in the studies.[81,82,122—124,126]

The paramagnetic dinuclear μ-N—C—S complexes of the "$g \approx 2.03$ family" (Fig. 6) with 5-amino-1,2,4-triazole-3-thiol, 1*H*-1,2,4-triazole-3-thiol, 1-methyltetrazole-5-thiol, and benzothiazole-2-thiol, which we have prepared[104,105] for the first time, are structurally different from the above-described compounds. The Fe(1) and Fe(2) atoms are linked to each other through the μ-N(3)—C(1)—S(1) and μ-N(3a)—C(1a)—S(1a) structural fragments characterized by the coordination mode IV (see Fig. 6). The iron atoms have tetrahedral configurations and are separated by a distance of 4.04 Å, unlike the dinuclear complexes, where Fe...Fe ≈ 2.7 Å.[81,82,124,125,127,128]

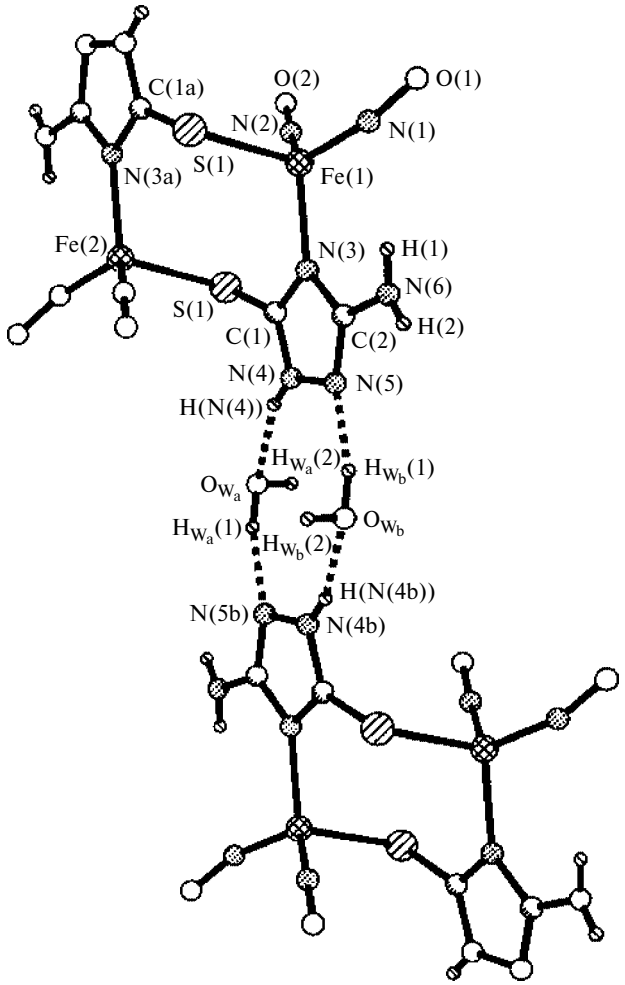

Fig. 6. Fragment of the crystal structure of $[Fe_2(SC_2H_3N_4)_2(NO)_4]\cdot 2H_2O$.

The dinuclear complexes are linked through intermolecular hydrogen bonds involving the W_a and W_b water molecules to form dimeric associates. The $H_{N(4)}$ atom of the triazole ring forms an intermolecular hydrogen bond with the oxygen atom of the W_a molecule ($H_{N(4)}...O_{W_a}$, 1.89 Å; $N(4)...O_{W_a}$, 2.82 Å; $N(4)—H_{N(4)}—O_{W_a}$, 169.1°), and the N(5) atom of the triazole ring forms an intermolecular hydrogen bond with the $H(1)_{W_b}$ atom ($N(5)...H(1)_{W_b}$, 2.08 Å; $N(5)...O_{W_b}$, 2.79 Å; $N(5)—H(1)_{W_b}—O_{W_b}$, 163.0°). The W_a and W_b molecules are not involved in hydrogen bonding with each other

(O_{W_a}...O_{W_b}, 4.47 Å). The $H(2)_{W_a}$ and $H(2)_{W_b}$ atoms are apparently disordered due to the twist of the hydrogen atom about the O_{W_a}—$H(1)_{W_a}$ and O_{W_b}—$H(1)_{W_b}$ bonds.

The Fe—S bond (2.305(1) Å) is ~0.04 Å longer than the bridging η^2-S Fe—S bonds in the thionate complexes with ligands **1** and **2** (2.280 and 2.262 Å, respectively).[124,125] The C—S bond (1.726(2) Å) is 0.04—0.05 Å shorter that the corresponding bonds in the complexes with ligands **1** and **2** (1.810 and 1.790 Å, respectively), which may be indicative of weakening of the Fe—S bond.[129,130] The Fe—N(3) bond between the iron atom and the nitrogen atom of the heterocyclic ligand in the paramagnetic dinuclear [Fe—S] nitrosyl complex is 2.020(2) Å. According to the published data,[131—134] the Fe—N bond in iron complexes is generally formed by a donor-acceptor mechanism and its length varies over a wide range depending on the oxidation state of the iron atom and the size of the heterocycle. A comparison of the bond lengths in the heterocycles of the complex with 5-amino-1,2,4-triazole-3-thiol provides evidence in favor of the coordination mode corresponding to the thione tautomeric form. After proton abstraction, the N(3) atom forms a Fe—N^- bond, and the S atom is involved in a donor-acceptor Fe←S bond. Analysis of the Fe—N—O structural fragments shows that they are essentially nonequivalent. The N—O and Fe—N bonds in the Fe—N(2)—O(2) fragment are shortened (N(2)—O(2), 1.156(3) Å; Fe—N(2), 1.677(2) Å) and this fragment is more linear (170.8(3)°). The N—O and Fe—N bonds in the Fe—N(1)—O(1) fragment are longer (N(1)—O(1), 1.174(3) Å; Fe—N(1), 1.695(2) Å), and the Fe—N(1)—O(1) angle (157.5(2)°) is the smallest of all the analogous angles in related complexes studied earlier[122,124,125] due apparently to the intermolecular Coulomb O(1)...S′ interaction. The difference in the Fe—N—O angles in this complex is 13.3°, as opposed to the dinuclear μ_2-S-substituted complexes, in which this difference is, on the average, 2—4°. In addition, the N(1)—Fe—N(2) angle (112.4(1)°) is 5—7° smaller than the analogous angles in the dinuclear complexes studied earlier.

In the neutral mononuclear [Fe—2S] dinitrosyl complex[103] with 1*H*-1,2,4-triazole-3-thiol, the iron atom is coordinated by two heterocycles and two NO groups (Fig. 7). The N(3) and N(6) atoms of the triazole rings are in the *syn* orientation with respect to the Fe atom. The triazole rings are linked through an intramolecular hydrogen bond (N(6)—H...N(3), 1.817(3) Å; N(6)...N(3), 2.715(3) Å; N(6)—H...N(3), 169.2(2)°). The Fe—S(1)—C(1)—N(3) and Fe—S(2)—C(3)—N(6) torsion angles (28.6° and −7.1°) are smaller than the Fe—S(1)—C(1)—N(4) and Fe—S(2)—C(3)—N(7) torsion angles (153.0° and 176.3°, respectively). The intramolecular Fe...N(3) and Fe...N(6) distances (3.439(2) and

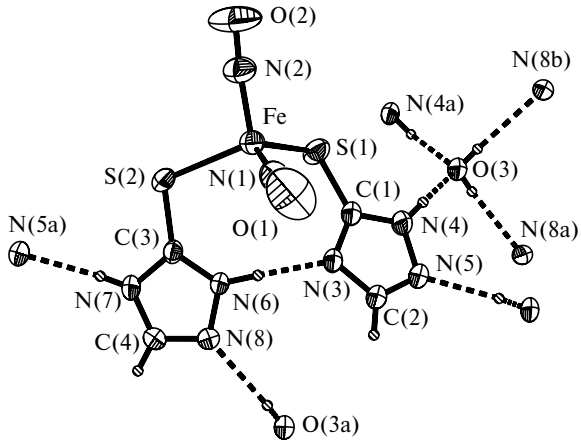

Fig. 7. Fragment of the crystal structure of $[Fe(SC_2H_3N_3)(SC_2H_2N_3)(NO)_2]\cdot 1/2\ H_2O$

3.446(2) Å, respectively) indicate that the iron atoms are not additionally coordinated by the nitrogen atoms of the rings. The main characteristic feature of the structure is that the heterocycles are coordinated to the iron atom in two modes, *viz.*, as the anionic ligand (in the thiol form) and the neutral ligand (in the thione form). This is confirmed by the difference in the C—S bond lengths (C(3)—S(2), 1.703(2) Å; C(1)—S(1), 1.725(2) Å) and the difference in the Fe—S bond lengths (Fe—S(1), 2.298(1) Å; Fe—S(2), 2.318(1) Å). The bond lengths and bond angles at the C(3) and C(1) atoms of two triazole rings are also noticeably different (C(3)—N(7), 1.353(3) Å; C(3)—N(6), 1.322(3) Å; C(1)—N(3), 1.333(3) Å; C(1)—N(4), 1.334(3) Å; N(7)—C(3)—N(6), 105.4°; N(3)—C(1)—N(4), 108.5°). An increase in the N(6)—N(8) bond length (1.375(2) Å) compared to the analogous N(4)—N(5) bond length in another ring (1.359(3) Å) can be attributable to the presence of the intramolecular N(6)—H...N(3) hydrogen bond. The differences in the geometric parameters of the rings are associated with the presence of intermolecular hydrogen bonds of three types: N(5)...H—N(7) (1.998(3) Å; N(5)...N(7), 2.776(3) Å; N(5)...H—N(7), 174.9(2)°); N(4)—H...O(3) (2.045 Å; O(3)...N(4), 2.876 Å; O(3)...H—N(4), 160.6°); and N(8)...H—O(3) (2.207 Å; O(3)...N(8), 2.938 Å; O(3)—H...N(8), 172.5°).

Spectroscopy of nitrosyl [Fe—S] complexes

With the aim of obtaining additional information on the structures of sulfur-containing iron nitrosyl clusters, a series of complex salts with various cations (including compounds, whose molecular and crystal structures are unknown), were studied by IR and Mössbauer spectroscopy (Table 4). The electron density on the M—NO bond (M is metal) can be adequately described[10] by three

Table 4. Parameters of the Fe^{57} Mössbauer spectra of [Fe—S] nitrosyl complexes at 85, 78,[a] and 296 K [b] and the average NO vibrational frequencies

Complex	Coordination unit	δ_{Fe}*	ΔE_Q**	Γ***	ν_{NO}	$\Delta\nu_{NO}$	Reference
		mm s^{-1}			cm^{-1}		
$(NH_4)[Fe_4(\mu_3\text{-}S)_3(NO)_7]\cdot H_2O$	$Fe_b\{S_2(NO)_2\}$	0.154	0.957	0.28	1738.7	—	76
	$Fe_a\{S_3(NO)\}$	0.158	0.733	0.24			
$(Bu^n_4)[Fe_4(\mu_3\text{-}S)_3(NO)_7]\cdot H_2O$	$Fe_b\{S_2(NO)_2\}$	0.141	0.894	0.30	1725.3	—	76
	$Fe_a\{S_3(NO)\}$	0.166	0.635	0.29			
$Na_2[Fe_2(\mu_2\text{-}S)_2(NO)_4]\cdot 4H_2O$	$Fe_b\{S_2(NO)_2\}$	0.091	0.510	0.28	1719.0	—	76
	$Fe_a\{S_2(NO)_2\}$	0.104	0.827	0.28			
$Cs_2[Fe_2S_2(NO)_4]\cdot 2H_2O$	$\{S_2(NO)_2\}$	0.078	0.368	0.27	1676.9	—	76
$\{Bu^n_4N\}_2[Fe_2S_2(NO)_4]\cdot 2H_2O$	$\{S_2(NO)_2\}$	0.064	0.258	0.27	1657.0	—	76
$Fe_4(\mu_3\text{-}S)_4(NO)_4$	$\{S_3(NO)\}$	0.150	1.473	0.334	—	—	134
$\{Me_4N\}_2[Fe_2(\mu_2\text{-}S_2O_3)_2(NO)_4]$	$Fe\{S_2(NO)_2\}$	0.163(1)[a]	1.241(1)[a]	0.28(3)[a]	1741, 1782	41	123
$\{Et_4N\}_2[Fe_2(\mu_2\text{-}S_2O_3)_2(NO)_4]$	$Fe\{S_2(NO)_2\}$	0.160(1)[a]	1.277(1)[a]	0.28(3)[a]	1745, 1771	26	123
$\{Pr^n_4N\}_2[Fe_2(\mu_2\text{-}S_2O_3)_2(NO)_4]$	$Fe\{S_2(NO)_2\}$	0.138(1)[a]	1.144(2)[a]	0.26(3)[a]	1746, 1772	26	123
$\{Bu^n_4N\}_2[Fe_2(\mu_2\text{-}S_2O_3)_2(NO)_4]$	$Fe\{S_2(NO)_2\}$	0.157(1)[a]	1.118(1)[a]	0.27(3)[a]	1750, 1770	20	123
$[Fe_2(SC_5H_4N)_2(NO)_4]$	$Fe\{SS(NO)_2\}$	0.177(1)	1.262(1)	0.320(2)	1734, 1792	58	125
$[Fe_2(S\,C_4H_3N_2)_2(NO)_4]$	$Fe\{SS(NO)_2\}$	0.169(1)	1.264(1)	0.290(2)	1748, 1797	49	126
$[Fe_2(SC_2H_3N_4)_2(NO)_4]\cdot 2H_2O$	$Fe\{SN(NO)_2\}$	0.304(1)	0.997(2)	0.305(2)	1732, 1805	73	105
		0.216(1)[b]	0.943(1)[b]	0.237(2)[b]			
$[Fe_2(C_2H_2N_3S)_2(NO)_4]\cdot H_2O$	$Fe\{SN(NO)_2\}$	0.293(1)	1.181(1)	0.329(2)	1732, 1805	73	105
		0.223(1)[b]	1.223(1)[b]	0.238(2)[b]			
$[Fe_2(C_2H_3N_4S)_2(NO)_4]\cdot H_2O$	$Fe\{SN(NO)_2\}$	0.298(1)	1.024(1)	0.260(2)	1732, 1794	75	105
		0.223(1)[b]	1.004(1)[b]	0.252(2)[b]			
$[Fe_2(C_7H_4NS_2)_2(NO)_4]\cdot H_2O$	$Fe\{SN(NO)_2\}$	0.291(1)	1.008(1)	0.258(2)	1729, 1790	62	105
		0.216(1)[b]	0.994(1)[b]	0.245(2)[b]			
$[Fe_2(C_7H_4N_2S)_2(NO)_4]\cdot H_2O$	$Fe\{SN(NO)_2\}$	0.287(1)	1.076(1)	0.290(2)	1725, 1802	77	135
$[Fe(SC_2H_3N_3)(SC_2H_2N_3)(NO)_2]\cdot 0.5H_2O$	$Fe\{SS(NO)_2\}$	0.188(1)[b]	1.118(1)[b]	0.258(2)[b]	1749, 1807	58	103
$(Et_4N)[Fe(SPh)_2(NO)_2]$	$Fe\{SS(NO)_2\}$	0.08[b]	0.78[b]	—	1744,1709	35	100

* The isomer shift with respect to α-Fe.
** Quadrupole splitting.
*** The line width.

forms, which exist depending on the nature of the metal atom and the ligands involved in its environment:

$$[M^{(n-1)+}\text{—}NO^+] \rightleftharpoons [M^{n+}\text{—}NO] \rightleftharpoons [M^{(n+1)+}\text{—}NO]$$
I II III

In the form I, the electron density is characterized by short M—NO bonds, high NO stretching frequencies (1650—1985 cm^{-1}), and electrophilic activity. The electron density of the form III is, on the contrary, characterized by an elongation of the M—NO bonds, a decrease in NO stretching frequencies (1525—1590 cm^{-1}), and nucleophilic activity. Moreover, the M—NO bonds are characterized by a variety of geometries (Fig. 8). The linear M—NO bond occurs either due to partial overlap of the occupied π orbital of NO and the unoccupied dz^2 orbital of the metal ion (NO serves as a σ-donor ligand) or due to π-back donation from the occupied dπ orbital of the metal ion to the antibonding π^* orbital of NO. This leads to destabilization of the dz^2 orbital (see Fig. 8). The angular M—NO bond occurs due to overlap of the dz^2 orbital and the π^* orbital of NO. This, to the contrary, stabilizes the dz^2 orbital.

In the [Fe—S] nitrosyl complexes (see Table 4), the NO stretching frequencies are in the 1657—1807 cm^{-1} region. Formally, the charge on the NO group can be taken equal to zero, *i.e.*, the iron atom is formally in the Fe(+1) state (d^7, S = 1/2). In this case, the bond angle at the apical iron atom in the tetranuclear anion is the most close to 180° (see Table 3). The Mössbauer spectra of the tetranuclear complexes with the $[Fe_4(NO)_7S_3]^-$ anion of the ammonium (Fig. 9, *a*) and tetrabutylammonium salts (Fig. 9, *b*) were processed as superpositions of two doublets with a fixed integral intensity ratio of 3 : 1 corresponding to the relative weights of two structurally nonequivalent iron positions, *viz.*, Fe_b and Fe_a, in the $[Fe_4(NO)_7S_3]^-$ anion, which differ in the formal charge and the composition of the coordination sphere. It should be noted that these parameters for the complex with the ammonium cation differ substantially (particularly, in the isomer shift for Fe_a, $\delta_a = 0.25$ m s^{-1}) from the parameters of the Mössbauer spectra of this complex, which have

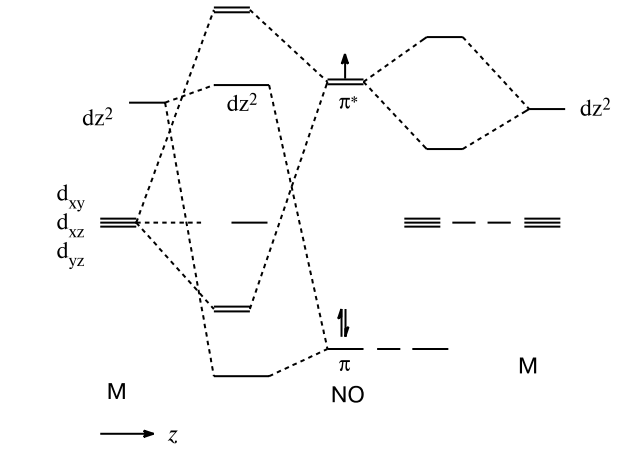

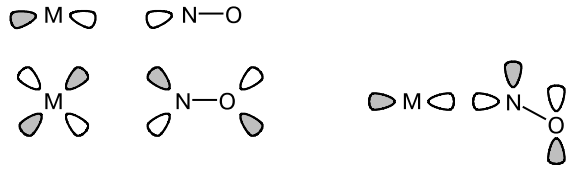

Geometry	Hybridization of nitrogen atom	ν(NO)/cm^{-1}
Linear M=N=O	sp	1650—1985
Angular M=N=O	sp^2	1525—1690
Bridging (μ_2-NO)	sp^2	~1500
(μ_3-NO)	sp^3	~1330

Fig. 8. Diagram of the molecular orbital of M—NO and the geometry of the M—NO bond.

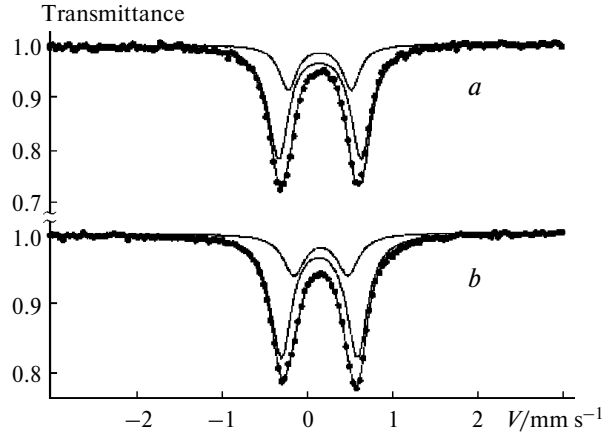

Fig. 9. Mössbauer spectra of the tetranuclear complexes with the $[Fe_4S_3(NO)_7]^-$ anion and the NH_4^+ (*a*) and $Bu^n{}_4N^+$ (*b*) cations.

been determined earlier[135] with the same ratio (3 : 1) of the relative contributions of Fe_b and Fe_a. Due to low spectral resolution, it is difficult to make an unambiguous choice between these two sets of parameters. The isomer shifts for Fe_a determined with the use of the chosen set of spectroscopic parameters are in the δ range for the equivalent states of the iron atoms in the neutral $[Fe_4(NO)_4S_4]$ complex.[135]

The Mössbauer spectrum of the sodium salt of the dinuclear complex with the $[Fe_2S_2(NO)_4]^{2-}$ dianion is adequately described as a superposition of two symmetrical quadrupole doublets (Fig. 10, *a*) with an intensity ratio of 1 : 1 provided that the line widths of individual doublets are equal. Taking into account this result and the X-ray diffraction data, it can be concluded that the iron positions in the dimer are structurally nonequivalent in spite of the identical composition of the coordination environment, $(\mu_2\text{-}S)_2(NO)_2$. On the contrary, the spectra of the dinuclear complexes with the cesium and tetrabutylammonium cations (see Fig. 10, *b*, *c*) are adequately described by one asymmetrical doublet with insignificantly broadened lines (see Table 4) in spite of the structural nonequivalence of the Fe atoms in the dimer of the cesium salt. The asymmetry of the lines in the absorption spectra *b* and *c* (see Fig. 10) is associated with a pronounced texture of samples, which were prepared as needle-like single crystals of different lengths, the axes of most crystals being located in the plane perpendicular to the direction of γ-quantum beam propagation.

Judging from the fact that the parameters of the ^{57}Fe Mössbauer spectra (see Table 4) depend substantially on the type of the cations in the crystals under investigation, the cations not only compensate the negative charge of the cluster but also affect substantially the structure of the cluster, *i.e.*, the bond angles and bond lengths. This influence is most pronounced in a

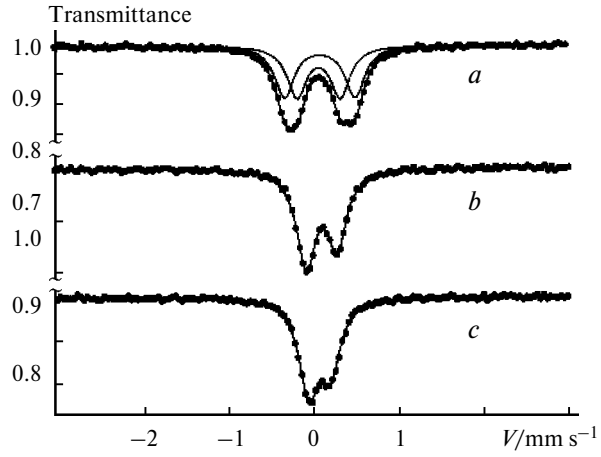

Fig. 10. Mössbauer spectra of the dinuclear complexes with the $[Fe_2S_2(NO)_4]^{2-}$ anion and the Na (*a*), Cs^+ (*b*), and $Bu^n{}_4N^+$ (*c*) cations.

series of crystals of the dinuclear complexes with the $[Fe_2S_2(NO)_4]^{2-}$ dianion. For example, ΔE_Q substantially decreases as the size of the cation increases, *i.e.*, the overall distribution of the valence-shell charges of the iron atom and the surrounding atoms becomes more symmetrical. This is surprising taking into account the difference in the composition of the nearest ligand environment of iron, $(\mu_2\text{-}S)_2(NO)_2$, and, apparently, a strong difference in the effective charges of the sulfur atoms and nitrosyl groups. The isomer shift also noticeably decreases with increasing size of the cation. This behavior is indicative of an increase in the s-electron density on the Fe^{57} nuclei from $A = Na^+$ to $A = Bu_4N^+$, as evidenced by a decrease in the Fe—S and Fe—Fe bond lengths. Actually, a tendency for shortening of the above-mentioned bonds is observed on going from the Me_4N^+ salt to the Cs^+ salt and is attributable to an increase in the degree of localization of the electron density on the bonding (relative to the Fe—Fe bonds) highest occupied molecular orbital of the dianion. Apparently, Me_4N^+ is more electrophilic than Cs^+ due to superconjugation. In turn, a decrease in the occupancy of the lowest unoccupied molecular orbital of the dianion composed primarily of the d orbitals of the Fe atom[129] should facilitate weakening of the $d\pi(Fe)\rightarrow\pi^*(NO)$ back donation and, correspondingly, lead to strengthening of the N—O bond.[128] This is confirmed by the observed decrease in the average NO stretching frequencies (1719.0 cm^{-1} for the sodium salt) by 42.1 and 62 cm^{-1} in the IR spectra of the Cs^+ and $Bu^n{}_4N^+$ salts, respectively.

Studies by Mössbauer spectroscopy demonstrated that the isomer shifts for the thiosulfate complexes are almost twice as large as those observed for the isoelectronic complexes with the $[Fe_2S_2(NO)_4]^{2-}$ anion (see Table 4). This suggests a decrease in the charge density on the iron atom, which is apparently associated with the electron-withdrawing properties of the SO_3 groups. In the thiosulfate complexes, the Fe—S bond lengths and the Fe—N—O angles tend to increase and the N—O bond lengths tend to decrease compared to the corresponding parameters in the sulfide complexes. Formally, the charge on the NO group can be considered as more positive compared to that in the sulfide anion. The parameters of the Mössbauer spectra of the μ_2-S-substituted complexes with the heterocyclic pyridine-2-thiol and pyrimidine-2-thiol ligands differ only slightly from those observed for the thiosulfate complexes (see Table 4).

For the nitrosyl μ-N—C—S complexes, the isomer shifts are almost twice as large as those observed for the complexes with structures of Roussin's red salt esters. This fact is indicative of a decrease in the 4s-electron density on the iron atom in the new type of complexes. Analysis of the Fe—N—O structural fragments in the μ-N—C—S complexes compared to those in the thionate μ_2-S complexes also revealed their nonequivalence. The N—O and Fe—N bonds in the Fe—N(2)—O(2) fragment are shorter (N(2)—O(2), 1.169(7) Å; Fe—N(2), 1.661(6) Å) and this fragment is more linear (171.5(6)°) compared to the Fe—N(1)—O(1) fragment, in which the N—O and Fe—N bonds are longer (N(1)—O(1), 1.187(7) Å; Fe—N(1), 1.681(5) Å) and the Fe—N—O angle (158.1(5)°) is the smallest of all the angles in the related complexes studied earlier. The difference in the Fe—N—O angles in the complex under consideration is 13.5°, in contrast to the μ_2-S-complexes, in which this difference is, on the average, 2—4°. Presumably, this difference in the structure of the iron nitrosyl fragments is attributable to the charge redistribution in the iron μ-N—C—S complexes so that one NO group becomes more positively charged. In the μ-N—C—S complexes, the Fe—N(2) bond (1.661(6) Å) is substantially shorter than another Fe—N bond (1.681(5) Å), and the Fe—N(2)—O(2) fragment is nearly linear (171.5(6)°). In the IR spectra of the new type of complexes, the stretching vibrations of nitrosyl groups are observed at high wavenumbers (see Table 4), the difference between two absorption bands is 73 cm^{-1}, whereas this difference for the μ_2-S complexes is 20—43 cm^{-1} (see Table 4). The observed substantial splitting of the bands is also, most likely, associated with the nonequivalence of the NO groups in the Fe—N—O fragments.

Magnetic properties of [Fe—S] nitrosyl complexes

On the assumption of the d^7 configuration of Fe(1+) and taking into account that the Fe...Fe distance is longer than 4 Å, the μ-N—C—S complexes would be expected to be paramagnetic. Actually, these complexes, unlike diamagnetic μ_2-S-substituted thiosulfate and thiolate complexes, give an ESR signal having a Lorentzian shape at $g \approx 2.032$ with a width of 6—10 mT. The number of unpaired electrons per iron atom, which was estimated based on measurements of the intensities of an ESR signal from a sample of a known weight, is 1.0±0.2. In fact, the $3d^7$ configuration in a tetrahedral coordination environment has the spin S = 3/2 formed by three unpaired electrons localized on dπ orbitals. However, we have to consider the total spin of the paramagnetic center formed by an individual Fe(d^7) ion (S = 3/2) in the dimer and two coordinated NO groups (S = 1/2). In the case of covalent bonding, every π^* electron of the NO group is paired with one dπ electron of Fe so that the total spin of the paramagnetic center is $S_t = 1/2$. The assumed electroneutrality of the NO groups implies that the electron pair of the bond is evenly shared by the Fe atom and the NO group. A shift of the electron pairs to the Fe atom results in the $Fe^{1-}(d^9)$—$2(NO^+)$ configuration. A shift of the electron pairs to the NO group gives rise to the $Fe^{3+}(d^5)$—$2(NO^{2-})$ configuration, the total spin $S_t = 1/2$

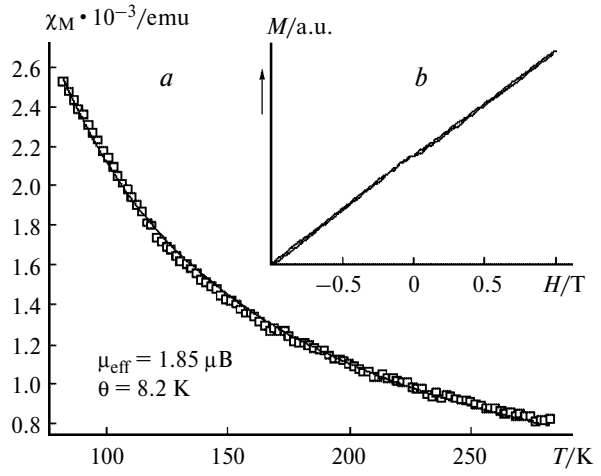

Fig. 11. *a*. Temperature dependence of the specific magnetic susceptibility of the dinuclear paramagnetic complex $[Fe_2(C_2H_3N_4S)_2(NO)_4] \cdot 2H_2O$. *b*. The dependence of the magnetization on the external magnetic field.

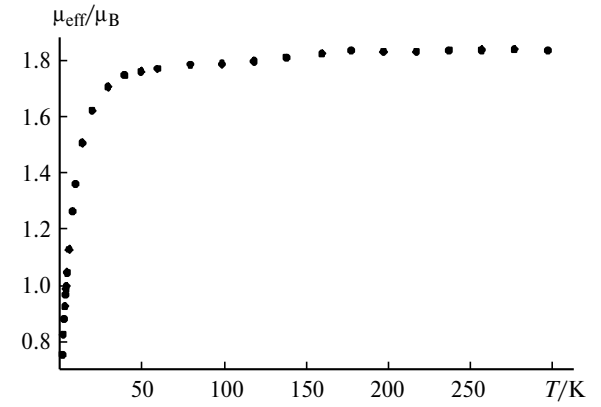

Fig. 12. Temperature dependence of the magnetic moment of $[Fe_2(C_2H_3N_4S)_2(NO)_4] \cdot 2H_2O$.

remaining unchanged. The magnetization of the complex depends linearly on the external magnetic field (Fig. 11, *b*), which indicates that there are no ferromagnetic impurities in the sample. The temperature dependence of the magnetic susceptibility (Fig. 12) is well described by the Curie—Weiss law with $\theta \cong 8$ K and the effective magnetic moment per Fe atom (μ_{eff}) equal to 1.85 μB. This value of μ_{eff} is approximately equal to the purely spin value for one unpaired electron (1.73). The absence of strong exchange interactions is consistent with a large distance between the iron atoms in this dinuclear complex.

In the mononuclear complex, the ligands exist in protonated and deprotonated forms. In the IR spectrum, the ligand existing in the thione form (**B**) appears as four thioamide bands located at 1570—1395 cm^{-1} (*I*), 1420—1260 cm^{-1} (*II*), 1140—940 cm^{-1} (*III*), and 800—700 cm^{-1} (*IV*).[136] These bands include primarily stretching (N=C) and bending (N—H) vibrations, the C=S stretching vibrations also making a substantial contribution to the intensities of these bands. The regions *I*—*III* of the IR spectrum of the mononuclear complexes show several absorption bands,[103] and only one band is observed in the region *IV* at 702 cm^{-1}. In the spectrum of the starting 1*H*-1,2,4-triazole-3-thione, this band is observed at 750 cm^{-1} or 745 cm^{-1}.[128] The large shift of the band in the region *IV* observed upon complex formation is indicative of a substantial weakening of the C=S bond and, consequently, a rather high strength of the S→Fe bond. This is consistent with the fact that the S→Fe and S—Fe bonds are similar in length. Presumably, the negative charge is localized on the S(1) atom due to deprotonation, and this atom forms a covalent bond with the iron atom.[136] Another sulfur atom, S(2), is formally neutral and is involved in a donor-acceptor bond with the iron atom.[128] The charge of the NO groups is close to zero. In the IR spectrum, the most intense absorption bands are assigned to NO vibrations (1807 and 1749 cm^{-1} with a shoulder at 1725 cm^{-1}). The Mössbauer spectrum of the complex has a doublet structure, and the parameters of the spectrum are larger than those observed for the isoelectronic anionic mononuclear complex[98] (see Table 4). Analysis of the main interatomic distances and angles in the neutral complex demonstrated that they are slightly different from the corresponding values in the anionic complex. A substantial increase in the isomer shift of the neutral mononuclear complex is apparently associated with an unusual coordination of 1*H*-1,2,4-triazole-3-thiol (STriaz) as the thione and thiolate ligands. An elongation of the Fe—$(STriaz)^-$ bonds compared to the Fe—$(SPh)^-$ bonds leads to a decrease in the 4s-electron density on the iron atom and, correspondingly, to an increase in the isomer shift. In addition, a weakening of σ-donation from the thione ligand to the iron atom, which is also associated with a decrease in the 4s-electron density on the iron nucleus, can also contribute to an increase in the isomer shift. A large asymmetry of the charge distribution around the iron atom in the $Fe^{+1}(S^0S^-NN)$ chromophore compared to $Fe^{+1}(S^-S^-NN)^-$ provides a qualitative explanation for an increase in ΔE_Q in the mononuclear neutral complex compared to the quadrupole splitting in the anionic mononuclear complex.

The mononuclear neutral complex is paramagnetic: the Fe...Fe′ distance in the complex is 5.225 Å. The ESR spectrum of a polycrystalline sample of the complex is characteristic of the axial anisotropy of the *g* factor ($g_\perp = 2.04$, $g_\parallel = 2.02$). At 100—300 K, the ESR line shape is temperature-independent. The temperature dependence of the second integral of the ESR spectrum follows the Curie law, and the ESR spectrum at half field was not observed. The single-crystal ESR spectrum of the complex shows a single line, whose *g* factor varies between $g_\perp$ and $g_\parallel$ depending on the orientation of the single crystal

relative to the magnetic field. The characteristic features of the ESR spectrum indicate that the spin of Fe in the molecular complex is 1/2. The temperature dependence of the magnetic susceptibility obeys the Curie law. According to the ESR data, the effective magnetic moment per iron atom is 1.77 μ_B, which is somewhat smaller than the theoretical value for the spin S = 1/2 (μ_{eff} = 1.73 μ_B), *i.e.*, it corresponds to 0.85 spin/complex.

In the solid state, the μ_2-S-substituted complexes are diamagnetic. At room temperature, the ESR spectra of solutions of the complexes with the thiosulfate anion have isotropic signals at $g_{aver} \approx 2.03$ with five-line hyperfine structures,[123] resulting from an interaction between the unpaired electron and two equivalent nitrogen nuclei of the NO ligands. This signal is identical to the signals of iron dinitrosyl complexes, which were found in microorganisms and animal tissues. It is believed that the action of nitrogen monoxide on the non-heme active sites of [2Fe—2S] and [4Fe—4S] proteins, resulting in inhibition of the active site of the protein or destruction of the active site and the formation of iron dinitrosyl complexes, is determined by the polarity of the medium *in vivo*. In this connection, investigations of the influence of the donor-acceptor properties of the solvents on the ESR parameters of all model $Fe_2(SR)_2(NO)_4$ complexes hold considerable promise.

Elimination of NO and N_2O from [Fe—S] nitrosyl complexes

The most intense peak in the spectrum of the gaseous phase[134] over an $Na_2[Fe_2(S_2O_3)_2]\cdot 4H_2O$ sample is observed at m/z = 18. This peak is assigned to the transfer of crystallization water from the complex to the gaseous phase. The second most intense peak is observed at m/z = 30. This peak is associated with the transfer of NO molecules to the gaseous phase on evacuation of the nitrosyl complex. What is surprising is that the spectrum has a rather intense peak at m/z = 44 associated with the presence of CO_2 or N_2O molecules in the gaseous phase. However, the presence of CO_2 molecules can be ruled out because of the virtual absence of the peak at m/z = 12 ($[C]^+$), which would be formed on irradiation of carbon dioxide molecules by electrons with energy of 70 eV. Consequently, we have to assume that vacuum decomposition is accompanied by elimination of not only NO but also N_2O. Irradiation of $Na_2[Fe_2(S_2O_3)_2]\cdot 4H_2O$ with ultraviolet light leads to a substantial increase in the intensity of the peak at m/z = 44 ($[N_2O^+]$), whereas the intensity of the peak at m/z = 30 ($[NO^+]$) decreases. Simultaneously, the intensity of the peak at m/z = 28 ($[N_2^+]$) increases. This effect (elimination of N_2O under irradiation) is most pronounced for the paramagnetic dinuclear complex $[Fe_2(SC_7H_5N_2)_2(NO)_4]$. A fragment of the IR spectrum of the gaseous phase over the

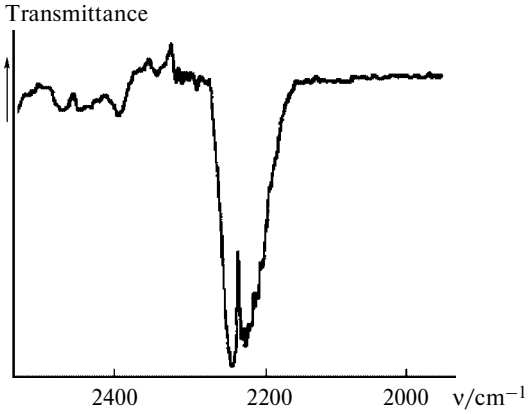

Fig. 13. The IR spectrum of the gaseous phase over the $[Fe_2(SC_7H_5N_2)_2(NO)_4]$ complex.

$[Fe_2(SC_7H_5N_2)_2(NO)_4]$ complex after its irradiation with UV light is shown in Fig. 13. The spectrum has a double absorption band (2235 cm^{-1}, a shoulder at 2010 cm^{-1}) characteristic of stretching vibrations of the triple bond in N_2O.[134]

It is known[44] that N_2O is one of the photolysis products of [Fe—S] nitrosyl complexes in inert solvents. The formation of non-heme iron dinitrosyl complexes $[Fe(NO)_2(SR)_2]^{2-}$ with various ligands in aqueous solutions in the absence of irradiation is also accompanied by elimination of N_2O.[137] In the presence of protons and an appropriate reducing agent, NO^- is readily transformed into nitroxyl, which then dismutates into N_2O and water:

$$2\,NO^- + 2\,H^+ \longrightarrow 2\,HNO \longrightarrow N_2O + H_2O.$$

The formation of N_2O in the absence of a reducing agent was explained[6] as follows. Initially, the NO groups in the complex undergo mutual redox transformations due to their coordination to the iron atom followed by the reaction of NO^- with the proton. However, this scheme is hardly applicable for explaining the solid-state photoreaction, because the involvement of the proton in this reaction is unlikely due to a large distance between the crystallization water molecules and the coordination sphere of the iron atoms. Moreover, this reaction is also observed for the $\{Pr^n_4N\}_2[Fe_2(\mu_2\text{-}S_2O_3)_2(NO)_4]$ complex[134] containing no proton-donor groups. Hence, an alternative mechanism should be assumed for the solid-phase formation of N_2O, which also operates in the presence of water of crystallization. Presumably, reduction of NO upon irradiation of these complexes proceeds through the intermediate state (IS):

$$Fe^{k+}(NO)_2 \xrightarrow{h\nu} IS \longrightarrow$$

$$\longrightarrow Fe^{(k+1)+}(N_2O_2)^- \longrightarrow Fe^{(k+2)+}O^{2-} + N_2O\uparrow.$$

The possibility of the formation of N_2O within the coordination sphere was examined[138] for the simplest repre-

Table 5. Distances (d) and angles (ω) in the $[Fe_2(NO)_4(\mu_2\text{-}S)_2]^{2-}$ complex calculated by the B3LYP method and experimental data

Parameter	Calculation		Experiment[103]
	LANL2DZ	6-31G*	
Bond		d/Å	
Fe—S	2.306	2.231	2.235, 2.243, 2.230, 2.240
Fe—N	1.628	1.600, 1.649	1.665, 1.654, 1.66, 1.675
N—O	1.240	1.200, 1.211	1.155, 1.17, 1.175, 1.148
Fe—Fe	2.749	2.601	2.703
Angle		ω/deg	
Fe—N—O	165.8	176.9, 143.9	165.4, 166.6, 167.9, 163.8
N—Fe—N	116.7	110.3	112.3, 144.9

sentative of the dinuclear $[Fe_2(NO)_4(\mu_2\text{-}S)_2]^{2-}$ complexes (**8**) by the density functional theory. The energies of intermediate structures formed in the course of transformations of two nitrosyl ligands into N_2O were calculated (Fig. 14). The calculated geometry of complex **8** is in rather good agreement with the experimental data (Table 5). The geometry optimization of complex **8** with the 6-31G* basis set gave a structure with the C_{2v} symmetry in contrast to the D_{2h} symmetry obtained in calculations with the LANL2DZ basis set,[76] which correlates better with the idealized geometry determined from X-ray diffraction data. When studying the possible intermediates in the reaction giving rise to N_2O, we changed symmetrically the coordination spheres of both Fe atoms to decrease the number of possible structures. Hence, the calculated change in the energy can be considered as approximately twice the change in the case of the corresponding transformation of only one center. The structure of the complex with N_2O (**9**) is very similar in energy to the structure of complex **8**. Taking into account a substantial nonlinearity of the NNO fragments (N—N—O, 140.3°) and an elongation of the N—O bond (1.318 Å), complex **9** can be considered as the $[Fe_2O_2S_2]$ complex with two N_2O^- species, which have an angular conformation in the isolated state (N—N—O, 133°; N—O, 1.369 Å).[139] Actually, the total charge on the NNO fragment (–0.61) is twice as large as the total charge on the NO fragment (–0.31) in complex **8**. However, the aver-

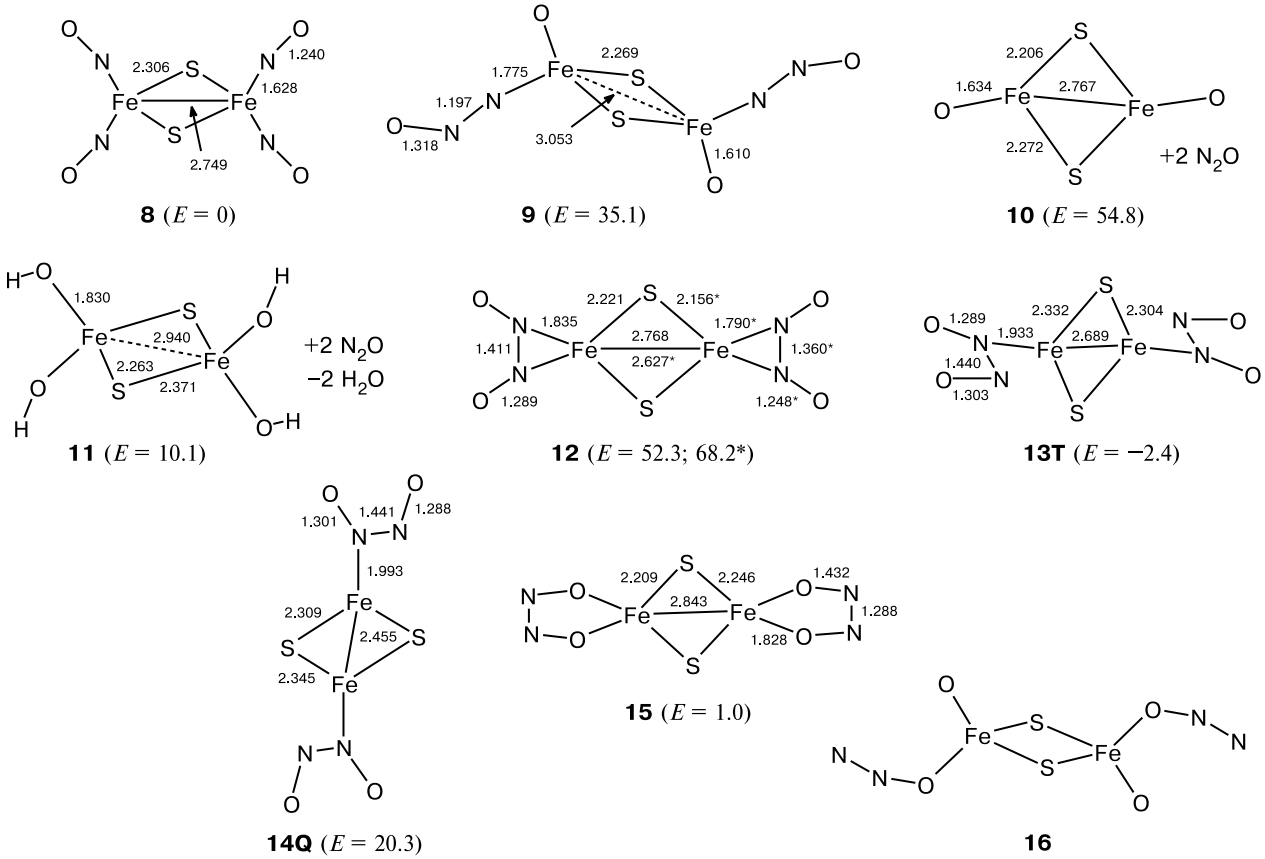

Fig. 14. Isomeric structures of the $[Fe_2(NO)_4(\mu_2\text{-}S)_2]^{2-}$ complex and the structures of the $[Fe_2(OH)_4(\mu_2\text{-}S)_2]^{2-}$ and $[Fe_2(O)_2\mu_2\text{-}S)_2]^{2-}$ complexes. The relative energies are given in kcal mol^{-1}, and the distances are given in Å.
* The values were calculated using geometry optimization with the 6-31G* basis set.

age energy of the Fe—N_2O bond cleavage (9.8 kcal mol^{-1}) in complex **9** is unexpectedly low. Taking into account the translational entropy of N_2O, the transformation **9** → **10** causes virtually no change in the free energy. In our opinion, such a low dissociation energy in spite of a very short Fe—N distance (1.775 Å) is attributable to the fact that the Fe atoms in the reaction product, *viz.*, complex **10**, are coordinatively unsaturated and form a bond, which is absent in compound **9**. The length of this bond (2.767 Å) is substantially smaller than the Fe—Fe distance (3.053 Å) in complex **9**. Apparently, the possibility of a change in the Fe—Fe bond length in dinuclear iron nitrosyl complexes upon their photoexcitation is essential for the formation of N_2O. For instance, we have recently demonstrated that N_2O was not eliminated from the mononuclear iron dinitrosyl complex in any noticeable amount under UV irradiation. The presence of a free coordination site after the removal of N_2O provides the possibility of coordinating the ligands present in the system. As a result, elimination of N_2O is a much more favorable process. As a model example, we calculated the structure of hydroxo complex **11** derived from **10** by the addition of two water molecules. In this case, the energy consumed in the reaction

8 + 2 H_2O = **11** + 2 N_2O

is as low as 10 kcal mol^{-1} (or 5 kcal mol^{-1}, on the average, per N_2O molecule).

A change in the N—Fe—N angle in complex **8** is sufficient for the formation of an N—N bond. The resulting singlet complex **12** exists as an equilibrium structure and its formation requires an energy of 26 kcal mol^{-1}, on the average, per metal center. Hence, from the thermodynamic point of view, this type of "doubling" of NO ligands would be expected to occur in primary photochemical processes. However, elucidation of the details of this process requires further experimental and theoretical investigations. The transformation **8** → **12** is accompanied by the electron density transfer (0.2 e) to the ONNO fragment, and its charge becomes equal to −0.80. The structure of **12** can be considered as a di-N-oxo π complex of molecular nitrogen or as a hyponitrite complex, where the hyponitrite ligand is coordinated in an unusual fashion through two N atoms. The usual coordination of the hyponitrite (structure **15**) is energetically more favorable (by 51 kcal mol^{-1}). This change in the coordination mode leads to shortening of the N—N bond from 1.411 to 1.288 Å and elongation of the N—O bond from 1.289 to 1.432 Å accompanied by a slight increase in the negative charge (to −0.90). As a result, the geometry of the ONNO fragment becomes rather similar to the geometry of the free $ONNO^{2-}$ dianion. The calculated[139] N—N and N—O bond lengths in the latter are 1.318 and 1.411 Å, respectively.

In the triplet and quintet states of **12**, coordination of the ONNO ligand is monodentate, which is accompanied by a noticeable decrease in the energy. The energies of the corresponding structures **13T** and **14Q** are 2.4 kcal mol^{-1} lower and 20.3 kcal mol^{-1} higher, respectively, than that of the starting complex **8**. Unrestricted open-shell calculations gave an even lower energy, a decrease being generally not very large. In this case, the orbitals of filled shells with upwards and downwards spins differ from each other much more substantially due to a radical change in the electronic structure. For example, three unpaired electrons on each iron atom in complex **14Q** are in a parallel orientation, the spin density is 2.87, and one unpaired electron on each ONNO ligand is in an antiparallel orientation with the spin density of −0.90. For other complexes with the zero full spin, each metal atom should also have a nonzero local spin density. For example, the tetrahedrally coordinated Fe^{III} center in the singlet complex **11** undoubtedly has a nonzero spin. Hence, its true electronic structure is a superposition of electronic configurations corresponding to two possible orientations of the localized spins Fe↑Fe↓ and Fe↓Fe↑. Calculations in a one-configuration approximation cannot adequately reproduce this effect and generally overestimate the energies of the states with S = 0 compared to the states with a nonzero spin. This is immediately evident from the calculated energies of the vertical singlet-triplet transitions in **8** and **12** (Table 6), which should in reality be small, be-

Table 6. Characteristics of the electronic structures of complexes **9** and **12** calculated by the B3LYP method with the LANL2DZ basis set

Complex	Spin density, S	E_{rel} /kcal mol^{-1}	Charges on atoms and groups			Spin density on atoms and groups		
			Fe	NO	ONNO	Fe	NO	ONNO
9	0	0	0.07	−0.30		—	—	—
9	1	−9.4	0.07	−0.35		2.59	−1.01	—
9	1*	21.8	0.03	−0.31		−0.12	0.55	—
12	0	0	0.04		−0.80	—		—
12	1	−6.1	0.13		−1.19	1.31		0.20

* An excited state with another spin structure, which was found with the use of a less precise convergence criterion.

cause they correspond to weak exchange interactions in a system with two magnetic centers. Table 6 also lists the characteristics of the excited triplet state with another spin structure. Presumably, complexes **12**, **13T**, and **14Q** are much more energetically similar than it follows from the results of calculations in a one-configuration approximation. Hence, it seems likely that the initially formed complex **12** is transformed first into **13T** or **14Q** and then into **9**. The first process occurs through a soft deformation mode of ONNO rotation in the coordination sphere of Fe and, hence, should has a low activation energy in thermal reactions. The subsequent process is analogous to α-elimination of the hydrogen atom, which generally readily occurs in the coordination sphere. However, the formation of hyponitrite complex **15** cannot be ruled out. Complex **15** is further transformed into complex **16**, in which the N_2O group is coordinated through the O atom, as a result of the cleavage of an elongated N—O bond.

Biological activities of [Fe—S] nitrosyl complexes

Considerable *adjuvant activity* of the dinuclear complexes in combination with antitumor cytostatics was revealed and studied. The addition of an NO donor of this class to cisplatin results in 100% survival in animals with leukemia P388 (individual therapy with cisplatin leads to 67% survival in animals). *Antimetastatic activity* of water-soluble μ_2-S complexes was demonstrated with melanoma B-16 and Lewis lung (LL) carcinoma. The preparations inhibit growth of a hypodermically implanted AKATOL tumor. The complexes synthesized exhibit[140] *vasodilatory activity*, their prolonged relaxant action was observed at concentrations of 10^{-6}—10^{-5} mol L^{-1}. Experiments were carried out on segments of rat thoracic aorta. The donation of nitrogen monoxide starts at a concentration of 10^{-6} mol L^{-1}, increases with increasing concentration of the complex to 10^{-5} mol L^{-1} and 10^{-4} mol L^{-1} (the percentage of vascular relaxation is 14.98, 50.26, and 60.40, respectively), and occurs without enzymatic activation and photoactivation. The complex spontaneously generates NO, which was detected *in vivo* using Fe-*N*-methyl-D-glucaminedithiocarbamate as a scavenger:[141]

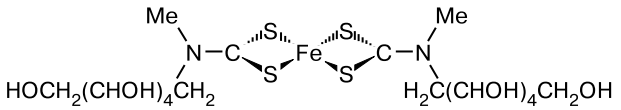

The genetic activity of the dinuclear iron tetranitrosyl complex with thiosulfate ($ITNC_{thio}$) $Na_2[Fe_2(\mu_2\text{-}S_2O_3)_2(NO)_4]\cdot 4H_2O$, the tetranitrosyl iron complex with aminotriazolethiol ($ITNC_{atria}$) $[Fe_2(SC_2H_3N_4)_2(NO)_4]\cdot 2H_2O$, and the mononuclear iron dinitrosyl complex with triazolethiol ($IDNC_{tria}$) $Fe(SC_2H_3N_3)(SC_2H_2N_3)(NO)_2]\cdot 0.5H_2O$ was studied in comparison with a solution of the mononuclear iron dinitrosyl complex with the natural ligand glutathione ($IDNC_{glu}$).[142] In systems of reparation of *Escherichia coli* DNA from oxidative (SoxRS) and alkylating (Ada) stresses, proteins controlling these processes serve simultaneously as chemosensors and transcription activators of regulon genes and contain potential NO targets with an iron sulfur center (SoxR [2Fe—2S] protein) or SH groups of cysteine residues in the functionally active C-terminal region (Ada protein). Functional activity of the above-mentioned molecular targets was controlled by an expression level of the corresponding genes. The NO complexes possess considerable genetic activity and exhibit rather low toxicity. For dinuclear $ITNC_{thio}$, the transcription activation of the SoxR gene involves the initial formation of the mononuclear dinitrosyl complex with $g = 2.032$. These results were confirmed by the data from ESR and mass-spectrometric analysis of aqueous solutions of $ITNC_{thio}$. The genetic activity of the complexes depends on the structure of the ligands. This effect was most pronounced in comparative experiments on Ada gene expression; Ada serves as a regulator of the adaptive response of cells to the known cancerolytic *N*-nitrosomethylurea. The use of $IDNC_{rglu}$ for cell adaptation to *N*-nitrosomethylurea led to a from two- to sevenfold enhancement of gene expression of an Ada regulon. A new phenomenon called "quasiadaptive response" was described. On the contrary, analogous experiments with $ITNC_{thio}$ led to essential sensitization of cells to cancerolytic *N*-nitrosomethylurea.

Conclusion

To summarize, the following adequate models of the active sites of [2Fe—2S] and [1Fe—2S] nitrosyl proteins were synthesized and characterized: diamagnetic sulfide, thiosulfate, and neutral μ_2-S-substituted complexes and paramagnetic neutral μ-S—C—N-bridged dinuclear and mononuclear [Fe—S] nitrosyl complexes. Procedures were developed for the synthesis of biologically active compounds containing simultaneously two functional fragments, *viz.*, the nitrosyl and thiol groups. In neutral mono- and dinuclear paramagnetic iron complexes with nitrogen-containing heterocyclic thiols, the electronic configuration of the metal—NO fragment $\{Fe(NO)_2\}^9$ can be proposed based on the results of X-ray diffraction analysis, ESR, Mössbauer, and IR spectroscopy. Stabilization conditions and magnetic properties of the complexes were studied in a broad temperature range. In the neutral complexes, the paramagnetic properties of the [Fe—SR,NO] center depend on the different tautomeric structures and the coordination mode of the RS-heterocyclic substituents, which offers considerable possibilities of varying the structure and properties of these complexes.

This study was financially supported by the Russian Foundation for Basic Research (Project No. 2-03-33344).

References

1. A. A. Nedospasov, *Biokhimiya*, 1998, **63**, 881 [*Biochemistry (Moscow)*, 1998, **63** (Engl. Transl.)].
2. D. A. Wink, M. Feelisch, J. Fukoto, D. Chistodoulou, M. B. Grisham, V. Vodovotz, J. A. Cook, M. Krishna, W. G. DeGraff, S. Kim, J. Gamson, and J. B. Mitchell, *Arch. Biochem. Biophys.*, 1998, **351**, 66.
3. I. Yu. Malyshev and E. B. Manukhina, *Biokhimiya*, 1998, **63**, 992 [*Biochemistry (Moscow)*, 1998, **63**, 840 (Engl. Transl.)].
4. N. J. Watmough, G. Butland, M. R. Cheesman, J. W. B. Moir, D. J. Richardson, and S. Spiro, *Biochim. Biophys. Acta*, 1999, **1411**, 456.
5. I. I. Severina, *Biokhimiya*, 1998, **63**, 939 [*Biochemistry (Moscow)*, 1998, **63**, 794 (Engl. Transl.)].
6. A. F. Vanin, *Biokhimiya*, 1998, **63**, 924 [*Biochemistry (Moscow)*, 1998, **63**, 731 (Engl. Transl.)].
7. C. L. Cammack, C. L. Joannou, X.-Y. Cui, S. R. Maray, C. T. Martinez, and M. N. Hughes, *Biophys. Biochem. Acta*, 1999, **1411**, 475.
8. M. Kelm, *Biochim. Biophys. Acta*, 1999, **1411**, 273.
9. E. B. Men´shchikova, N. K. Zenkov, and V. P. Reutov, *Biokhimiya*, 2000, **65**, 485 [*Biochemistry (Moscow)*, 2000, **65**, 409 (Engl. Transl.)].
10. M. Fontecave and J.-L. Pierre, *Bull. Soc. Chem. Fr.*, 1994, **131**, 620.
11. S. Bian and J. A. Cowan, *Coord. Chem. Rev.*, 1999, **190**, 1049.
12. R. Butler and I. L. Megson, *Chem. Rev.*, 2002, **102**, 1155.
13. A. R. Butler and P. Rhodes, *Anal. Biochem.*, 1997, **249**, 1.
14. B. Gaston, *Biochim. Biophys. Acta*, 1999, **1411**, 323.
15. A. R. Butler, S. Elkins-Daukes, D. Parkin, D. Lyn, and H. Williams, *Chem. Commun.*, 2001, 1732.
16. D. A. Wink and J. B Mitchell, *Free Radical Biol. Medicine*, 1998, **25**, 434.
17. S. G. Lloyd, R. Franco, J. J. G. Moura, I. Moura, G. C. Ferreira, and B. H. Huynh, *J. Am. Chem. Soc.*, 1996, **118**, 9892.
18. N. V. Voevodskaya, L. N. Kubrina, V. A. Serezhenkov, V. D. Mikoyan, and A. F. Vanin, *Curr. Topics Biophys.*, 1999, **23**, 31.
19. B. D´Autreaux, *Proc. Nat. Acad. Sci. USA*, 2002, **99**, 16619.
20. M. S. Koo, *EMBO J.*, 2003, **22**, 2614.
21. S. Constanco, S. Menage, R. Purrello, R. P. Bonomo, and M. Fontecave, *Inorg. Chim. Acta*, 2001, **318**, 1.
22. A. F. Vanin, V. A. Serezhenkov, V. D. Mikoyan, and M. V. Genkin, *Nitric Oxide: Biol. Chem.*, 1998, **2**, 224.
23. P. G. Wang, M. Xian, and X. P. Tang, *Chem. Rev.*, 2002, **102**, 1091.
24. N. Reginato, C. T. C. McCrory, and D. Pervitsky, *J. Am. Chem. Soc.*, 1999, **121**, 10217.
25. R. Basosi, E. Gaggelli, and E. Tiezzi, *J. Chem. Soc., Perkin Trans. 2*, 1975, 423.
26. I. S. Severina, O. G. Bussygina, N. V. Pyatakova, I. V. Malenkova, and A. F. Vanin, *Nitric Oxide*, 2003, **8**, 155.
27. P. K. Mascharak, *Coord. Chem. Rev.*, 2002, **225**, 201.
28. S. Nagashima, M. Nakasako, N. Dohmae, M. Tsujimura, K. Takio, M. Odaka, M. Yohda, N. Kamiya, and I. Endo, *Nat. Struct. Biol.*, 1998, **5**, 347.
29. G.-M. Rinanese, F. De Angelis, S. Melchionna, and A. De Vita, *J. Am. Chem. Soc.*, 2000, **122**, 11963.
30. M. Lo Bello, M. Nuccetelli, A. M. Caccuri, L. Stella, M. W. Parker, J. Rossjohn, W. J. McKinstry, A. F. Mozzi, G. Federici, F. Polizio, J. Z. Pedersen, and G. Ricci, *J. Biol. Chem.*, 2001, **276**, 42138.
31. P. Turella, *J. Biol. Chem.*, 2003, **278**, 42294.
32. K. J. Reszka, Z. Matuszak, C. F. Chignell, and J. Dillon, *Free Radical Biol. Medicine*, 1999, **26**, 669.
33. H. Beinert, *J. Biol. Inorg. Chem.*, 2000, **5**, 2.
34. M. Feelisch, *Naunyn-Schmiedeberg´s Arch. Pharmacol.*, 1998, **358**, 113.
35. J.-L. Burgaud, E. Ongini, and P. Del Soldato, *Ann. N. Y. Acad. Sci.*, 2002, **962**, 360.
36. J. Bourassa, W. DeGraff, and S. Kudo, *J. Am. Chem. Soc.*, 1997, **119**, 2853.
37. R. V. Blackburn, S. S. Galoforo, C. M. Berns, N. M. Motwanu, P. M. Corry, and Y. J. Lee, *Cancer*, 1998, **82**, 1137.
38. J. L. Williams, *Cancer Res.*, 2001, **61**, 3285.
39. A. L. Kleschov, G. Hubert, T. Munzel, C. Stoclet, and B. Bucher, *BMC Pharmaclol.*, 2002, **2**, 3.
40. Y. M. Kim, H. T. Chung, R. L. Simmons, and T. R. Billar, *J. Biol. Chem.*, 2000, **275**, 10954.
41. T. R. Bryar and D. R. Eaton, *Can. J. Chem.*, 1992, **70**, 1917.
42. D. A. Wink, Y. Vodovotz, J. A. Cook, M. C. Krishna, S. Kim, D. Coffin, and J. B Mitchell, *Biokhimiya*, 1998, **63**, 948 [*Biochemistry (Moscow)*, 1998, **63**, 802 (Engl. Transl.)].
43. F. W. Flitney, I. L. Megson, J. L. M. Thomson, G. D. Kennovin, and A. R. Butler, *Brit. J. Pharmacol.*, 1996, 117.
44. P. C. Ford, J. Bourassa, S. Kudo, and K. Miranda, *Coord. Chem. Rev.*, 1998, **171**, 185.
45. T. Ueno, Y. Suzuki, and S. Fujii, *Biochem. Pharmacol.*, 2002, **63**, 485.
46. T. Taylor, I. W. Taylor, L. F. Chasseaud, and R. Bonn, *Prog. Drug Metab.*, 1987, **10**, 207.
47. K. E. Torfgard and J. Ahlner, *Cardiovasc. Drugs Ther.*, 1994, **8**, 701.
48. S. Ya. Proskuryakov, A. G. Konoplyannikov, A. I. Ivannikov, V. G. Skvortsov, and A. F. Tsyb, *Ross. Onkologich. Zh.* [*Russ. J. Oncology*], 2000, No. 3, 41 (in Russian).
49. G. Rossoni, *J. Farmacol. Exp. Ther.*, 2001, **297**, 380.
50. V. G. Granik and N. B. Grigor´ev, *Izv. Akad. Nauk, Ser. Khim.*, 2002, 1268 [*Russ. Chem. Bull., Int. Ed.*, 2000, **49**, 1375].
51. L. K. Keefer, J. L. Flippen-Anderson, C. George, A. P. Shanklin, T. M., D. Christodoulou, J. E. Saavedra, E. S. Sagan, and D. Scott-Bohl, *Nitric Oxide: Biol. Chem.*, 2001, **5**, 377.
52. L. K. Keefer, R. N. Nims, K. M. Davies, and D. A. Wink, *Methods Enzymol.*, 1996, **268**, 281.
53. A. L. Fitzhugh and L. K. Keefer, *Free Radical Biol. Medicine*, 2000, **28**, 1463.
54. C. M. Maragos, D. Morley, D. A. Wink, T. M. Duanams, J. E. Saavedra, A. Hoffman, A. A. Bove, L. Isaac, J. A. Hrabie, and L. K. Keefer, *J. Med. Chem.*, 1991, **34**, 3242.

55. A. Mulsch, M. Hecker, P. I. Mordvincev, and A. F. Vanin, *Naunyn-Schmiedeberg´s Arch. Pharmacol.*, 1993, **347**, 92.
56. E. Noack and M. Feelisch, *J. Cardiovasc. Pharmacol.*, 1989, **14**, 1.
57. M. Feelisch, J. Ostrowski, and E. Noack, *J. Cardiovasc. Pharmacol.*, 1989, **14**, 13.
58. J. Oszajca, G. Stochel, E. Wasielewska, Z. Stasicka, R. J. Gryglewski, A. Jakubowski, and K. Gieslik, *J. Inorg. Biochem.*, 1998, **69**, 121.
53. A. R. Butler, F. W. Flitney, and D. L. H. Williams, *Trends Pharmacol. Sci.*, 1995, **16**, 18.
59. J. N. Bates, M. T. Baker, R. Jr. Guerra, and D. G. Harrison, *Biochem. Pharmacol.*, 1991, **42**, 157.
60. R. V. Blackburn, S. S. Galoforo, C. M. Berns, C. V. Motwani, P. M. Corry, and Y. J. Lee, *Cancer*, 1998, **82**, 1137.
61. M. Clarke and J. B. Caul, *J. Inorg. Chem.*, 1993, **32**, 147.
62. D. R. Lang, J. A. Davis, L. G. F. Lopes, A. A. Ferro, L. C. G. Vasconcellos, D. W. Franco, E. Tffouni, A. Wieraszco, and M. Carke, *J. Inorg. Chem.*, 2000, **39**, 2294.
63. V. G. Granik and N. B. Grigor´ev, *Oksid azota (NO)* [*Nitric Oxide (NO)*], Vuzovskaya kniga, Moscow, 2004, 63 pp. (in Russian).
64. K. Lala, *Cancer and Metastasis Rev.*, 1998, **17**, 1.
65. K. Kabisov, V. V. Sokolov, A. B. Shekhter, A. V. Pekshev, and M. V. Maneilova, *Ross. Onkologich. Zh.* [*Russ. J. Oncology*], 2000, No. 1, 24 (in Russian).
66. A. Janczyk, A. Wolnicka-Glubisz, A. Chmura, M. Elas, Z. Matuszak, G. Stochel, and K. Urbanska, *Nitric Oxide*, 2004, **10**, 42.
67. O. Siri, A. Tabard, P. Pullumbi, and R. Guilard, *Inorg. Chim. Acta*, 2003, 633.
68. S. Ya. Proskuryakov, S. I. Biketov, A. I. Ivannikov, and V. G. Skvortsov, *Immunologiya* [*Immunology*], 2000, **1**, 9 (in Russian).
69. A. F. Vanin, R. A. Stukan, and E. B. Manukhina, *Biochim. Biophys. Acta*, 1996, **1295**, 5.
70. E. Masini, D. Salvemini, J. F. Ndisang, P. Gai, L. Berni, M. Moncini, S. Bianchi, and P. F. Mannaioni, *Inflamm. Res.*, 1999, **48**, 561.
71. H. Preiser, *Sepsis*, 2000, **4**, 99.
72. F. Z. Roussin, *Ann. Chim. Phys.*, 1858, **52**, 285.
73. A. R. Butler, C. Glidewell, and M.-H. Li, *Adv. Inorg. Chem.*, 1988, **32**, 335.
74. F. W. Flitney, I. L. Megson, D. E. Flitney, and A. R. Butler, *Brit. J. Pharmacol.*, 1992, **107**, 842.
75. J. L. Bourassa and P. C. Ford, *Coord. Chem. Rev.*, 2000, **200**, 887.
76. N. A. Sanina, I. I. Chuev, S. M. Aldoshin, N. S. Ovanesyan, V. V. Strelets, and Yu. V. Geletii, *Izv. Akad. Nauk, Ser. Khim.*, 2000, **49**, 443 [*Russ. Chem. Bull., Int. Ed.*, 2000, **49**, 444].
77. J. T. Thomas, J. H. Robertson, and E. G. Cox, *Acta Crystallogr.*, 1958, **11**, 599.
78. A. R. Butler, C. Glidewell, A. R. Hyde, and J. McGinnis, *Inorg. Chem.*, 1985, **24**, 2931.
79. S. S. Sung, C. Glidewell, A. R. Butler, and R. Hoffman, *Inorg. Chem.*, 1985, **24**, 3856.
80. C. Glidewell, M. E. Harman, M. B. Hursthouse, I. L. Johnson, and M. Motevali, *J. Chem. Research (S)*, 1988, 212.
81. A. R. Butler, C. Glidewell, and S. Glidewell, *Polyhedron*, 1990, **9**, 2399.
82. K. A. Hofmann and O. F. Wiede, *Z. Anorg. Allg. Chem.*, 1895, **9**, 295.
83. C. Glidewell, R. J. Lambert, M. E. Harman, and M. B. Hursthouse, *J. Chem. Soc., Dalton Trans.*, 1989, 2061.
84. O. A. Rakova, N. A. Sanina, G. V. Shilov, V. V. Strelets, I. B. Borzova, A. V. Kulikov, and S. M. Aldoshin, *Koord. Khim.,* 2001, **27**, 698 [*Russ. J. Coord. Chem.*, 2001, **27**, 657 (Engl. Transl.)].
85. C. Glidewell, R. J. Lambert, M. E. Harman, and M. B. Hursthouse, *J. Chem. Soc., Dalton Trans.*, 1990, 2685.
86. G. Brauer, *Handbuch der Preparativen Inorganischen Chemie*, Enke, Stuttgart, 1960, **2**, 1526.
87. T. B. Rauchfuss and T. D. Weatherill, *Inorg. Chem.*, 1982, **21**, 827.
88. G. Martini and E. Tiezzi, *Z. Naturforsch.*, 1973, **28b**, 300.
89. C. L. Conrado, J. L. Bourassa, C. Egler, S. Wecksler, and P. C. Ford, *Inorg. Chem.*, 2003, **42**, 2288.
90. I. I. Lobysheva, V. A. Serezhenkov, R. A. Stukan, M. K. Bouman, and A. F. Vanin, *Biokhimiya*, 1997, **62**, 934 [*Biochemistry (Moscow)*, 1997, **62**, 801 (Engl. Transl.)].
91. M. V. Stupakova, I. I. Lobysheva, V. D. Mikojan, A. F. Vanin, and S. V. Vasil´eva, *Biochemistry (Moscow)*, 2000, **65**, 810.
92. A. Mulsch, P. I. Mordvincev, A. F. Vanin, and R. Buss, *FEBS Lett.*, 1991, **294**, 252.
93. I. Y. Malyshev, A. V. Malugin, L. Y. Golubeva, T. A. Zenina, E. B. Manukhina, V. D. Mikoyan, and A. F. Vanin, *FEBS Lett.*, 1996, **391**, 21.
94. I. S. Severina, O. G. Bussygina, N. V. Pyatakova, I. V. Malenkova, and A. F. Vanin, *Nitric Oxide*, 2003, **8**, 155.
95. A. F. Vanin, B. Muller, J. L. Alencar, I. I. Lobysheva, F. Nepveu, and J.-C. Stoclet, *Nitric Oxide*, 2002, **7**, 194.
96. A. F. Vanin, B. Muller, J. L. Alencar, I. I. Lobysheva, F. Nepveu, and J.-C. Stoclet, *Curr. Top. Biophys.*, 2002, **26**, 101.
97. L. Li, J. R. Morton, and K. F. Preston, *Magnet. Reson. Chem.*, 1995, **33**, S14.
98. H. Strasdeit, B. Krebs, and G. Henkel, *Z. Naturforsch.*, 1986, **41B**, 1357.
99. K. M. Bultusis, K. D. Karlin, H. N. Rabinowitz, J. C. Dewan, and S. J. Lippard, *Inorg. Chem.*, 1980, **19**, 2627.
100. Ch.-Yi Chiang, M. L. Miller, J. H. Reibenspies, and M. Y. Darenbourg, *J. Am. Chem. Soc.*, 2004, **126**, 10867.
101. A. F. Vanin, R. A. Stukan, and Y. B. Manukhina, *Biophysics*, 1997, **42**, 7.
102. C. V. Vasil´eva, M. V. Stupakova, I. I. Lobysheva, V. D. Mikoyan, and A. F. Vanin, *Biokhimiya*, 2001, **66**, 1209 [*Biochemistry (Moscow)*, 2001, **66**, 984 (Engl. Transl.)].
103. N. A. Sanina, O. A. Rakova, S. M. Aldoshin, G. V. Shilov, Yu. M. Shulga, A. V. Kulikov, and N. S. Ovanesyan, *Mendeleev Commun.*, 2004, **14**, 7.
104. O. A. Rakova, N. A. Sanina, S. M. Aldoshin, N. A. Goncharova, G. V. Shilov, Yu. M. Shulga, and N. S. Ovanesyan, *Inorg. Chem. Commun.*, 2003, **6**, 145.
105. S. M. Aldoshin, N. A. Sanina, O. A. Rakova, G. V. Shilov, A. V Kulikov, Yu. M. Shul´ga, and N. S. Ovanesyan, *Izv. Akad. Nauk, Ser. Khim.*, 2003, 1614 [*Russ. Chem. Bull., Int. Ed.*, 2003, **52**, 1702].
106. E. S. Raper, *Coord. Chem. Rev.*, 1997, **165**, 475.

107. E. S. Raper, *Coord. Chem. Rev*., 1985, **61**, 115.
108. P. D. Akrivos, *Coord. Chem. Rev*., 2001, **213**, 181
109. H. De. Wewer, P. Besse, and H. Verachtert, *Appl. Microbiol. Biotechnol*., 1994, **42**, 631.
110. U. Abram, J. Mack, K. Ortner, and M. Muller, *J. Chem. Soc., Dalton Trans*., 1998, 1011.
111. R. W. Klark, P. J. Squattrito, A. K. Sen, and S. N. Dubey, *Inorg. Chim. Acta*, 1999, **293**, 61.
112. C. M. Menzies and P. J. Squattrito, *Inorg. Chim. Acta*, 2001, **314**, 194.
113. I. V. Tsarenko, A. V. Makarevich, and D. A. Orechov, *Bio. Eng*., 1998, **19**, 469.
114. G. Cervantes, S. Marchal, and M. J. Prieto, *J. Inorg. Biochem*., 1999, **77**, 197.
115. M. Mazzo, V. Cherch, and M. Nicolini, *Farmaco*, 1993, **48**, 1631.
116. V. M. Gonzalez, M. A. Fuertes, M. J. Perez-Alvarez, G. Cervantes, V. Moreno, C. Alonso, and J. M. Perez, *Biochem. Pharmacol*., 2000, **60**, 371.
117. S. G. Rosenfield, P. K. Mascharak, and S. K. Arora, *Inorg. Chim. Acta*., 1987, **129**, 39.
118. G. Johansson and W. N. Lipscomb, *Acta Crystallogr*., 1958, **11**, 594.
119. C. T.-W. Chu and L. F. Dah, *Inorg. Chem*., 1977, **16**, 3245.
120. X. Lin, A. Zheng, Sh. Lin, J. Huang, and J. Lu, *J. Struct. Chem. (Wuhan)*, 1982, **1**, 79.
121. L. Huang, X. Zhao, B. Zhuang, and H. Jiegon, *J. Struct. Chem. (Wuhan)*, 1992, **11**, 397.
122. N. A. Sanina, O. A. Rakova, S. M. Aldoshin, I. I. Chuev, E. G. Atovmyan, and N. S. Ovanesyan, *Koord. Khim.,* 2001, **27**, 198 [*Russ. J. Coord. Chem*., 2001, **27**, 179 (Engl. Transl.)].
123. N. A. Sanina, O. S. Filipenko, S. M. Aldoshin, and N. S. Ovanesyan, *Izv. Akad. Nauk, Ser. Khim*., 2000, 1115 [*Russ. Chem. Bull., Int. Ed*., 2000, **49**, 1109].
124. O. A. Rakova, N. A. Sanina, G. V. Shilov, Yu. M. Shulga, V. M. Martynenko, N. S. Ovanesyan, and S. M. Aldoshin, *Koord. Khim.,* 2002, **28**, 364 [*Russ. J. Coord. Chem*., 2002, **28**, 341 (Engl. Transl.)].
125. O. A. Rakova, N. A. Sanina, S. M. Aldoshin, Yu. M. Shulga, and A. V. Kulikov, *J. Inorg. Biochem*., 2001, **89**, 390.
126. T. C. W. Mak, L. Book, C. Chien, M. K. Gallagher, L. C. Song, and D. Seyferth, *Inorg. Chim. Acta*., 1983, **73**, 159.
127. J. D. Baty, R. G. Willis, and M. G. Burdon, *Inorg. Chim. Acta*, 1987, **138**, 15.
128. A. K. Sen, R. N. Singh, and R. N. Handa, *J. Mol. Struct*., 1998, **470**, 61.
129. J. Jolley, W. I. Cross, and R. G. Pritchard, *Inorg. Chim. Acta*, 2001, **315**, 36.
130. D. H. Templeton, A. Zalkin, and T. Ueki, *Acta Crystallogr., Sect. A*, 1966, **21**, 154.
131. I. A. Latham, G. J. Leigh, and C. J. Pickett, *J. Chem. Soc. Dalton Trans*., 1986, 1986.
132. E. Konig and K. J. Watson, *Chem. Phys. Lett*., 1970, **6**, 457.
133. E. Kostiner, J. Steger, and J. R. Rea, *Inorg. Chem*., 1970, **9**, 1939
134. O. A. Rakova, N. A. Sanina, Yu. M. Shulga, V. M. Martynenko, N. S. Ovanesyan, and S. M. Aldoshin, *Dokl. Akad. Nauk,* 2002, **383**, 350 [*Dokl. Chem*., 2002, **383**, 1—3, 75 (Engl. Transl.)].
135. C. T.-W. Chu, F. Y. K. Lo, and L. F. Dahl, *J. Am. Chem. Soc*., 1982, **104**, 3409.
136. O. Jimenez-Sandoval, R. Cea-Olivares, and S. Hernandez-Ortega, *Polyhedron*, 1997, **16**, 4129.
137. K. A. Pearsall and F. T. Bonner, *Inorg. Chem*., 1982, **21**, 1973.
138. A. F. Shestakov, S. M. Aldoshin, N. A. Sanina, and Yu. M. Shulga, *Mendeleev Commun*., 2004, **14**, 1.
139. A. F. Shestakov and A. E. Shilov, *Izv. Akad. Nauk, Ser. Khim*., 2001, 1963 [*Russ. Chem. Bull., Int. Ed*., 2001, **50**, 2054].
140. N. A. Sanina, O. A. Rakova, S. M. Aldoshin, N. P. Konovalova, and E. V. Manukhina, *Abstrs of Papers, Intern. Symp. on Reactive Oxygen and Nitrogen Species: Diagnostic, Preventive and Therapeutic Values*, St. Petersburg, 2002, 188.
141. A. Komarov, D. Mattson, M. M. Jones, P. K. Singh, and Ch.-S. Lai, *Biochem. Biophys. Res. Commun*., 1993, **195**, 1191.
142. S. V. Vasil´eva, E. Yu. Moshkovskaya, N. A. Sanina, S. M. Aldoshin, and A. F. Vanin, *Biokhimiya*, 2004, **69**, 1088 [*Biochemistry (Moscow)*, 2004, **69**, 883 (Engl. Transl.)].

Received June 28, 2004;
in revised form October 27, 2004